9-10-2010

The development of a modified biaxial composite test specimen

Anthony Torres

Anthony Torres
Candidate

Civil Engineering
Department

This thesis is approved, and it is acceptable in quality and form for publication:

Approved by the Thesis Committee:

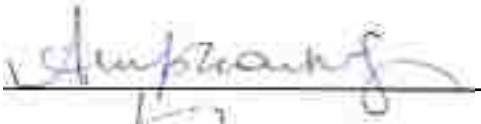

Dr. Arup Maji , Chairperson

Dr. Rafiqul Tarefder

Hans-Peter Dumm

THE DEVELOPMENT OF A MODIFIED BI-AXIAL COMPOSITE TEST SPECIMEN

BY

ANTHONY SAMUEL TORRES

B.S., Civil Engineering, New Mexico State University, 2008

THESIS

Submitted in Partial Fulfillment of the
Requirements for the Degree of

Masters of Science
Civil Engineering

The University of New Mexico
Albuquerque, New Mexico

May, 2010

DEDICATIONS

This thesis is dedicated to my wife Allison for always being there for me and to my ferocious little Yorkie Hannibal. He always cheered me up when I needed it.

ACKNOWLEDGEMENTS

First and foremost, I wouldn't have even made it this far in my education had it not have been for my loving wife Allison. From the moment I met her, she changed the way I viewed the world of knowledge and understanding. She encouraged me to not set limits on what I can learn in life and to always allow my mind to grow. She had to endure countless practice presentations and read/edited many drafts of this very research. She knows almost as much as I do now. I am eternal grateful for her love and support.

This research would have not been possible without the help of everyone at the Air Force Research Laboratory, Kirtland AFB, New Mexico. Lee Underwood and Gerry Geil both took time out of their busy schedule to help me fabricate all of my composite panels as well teaching me things I simply wouldn't have been able to learn from any textbook. I wouldn't know as much about composites today hadn't of been for them. Also, Adam Biskner deserves a world of gratitude for all the time I spent in his office bugging him about the world of bi-axial testing. Without Adam's help there simply wouldn't be any bi-axial data to analyze. Marty and Mike also deserve a special thanks for allowing me to sneak in a few more panels to machine. Without their help I wouldn't have had my new specimens. Another big thanks to everyone at AFRL who helped in any way whatsoever.

Thank you to Dr. Arup Maji for being my advisor and thesis chair for this research and also being there to make sense of things when I couldn't seem to. Thank you for your support and guidance outside of this research as well.

A thank you to my advisor and committee member Hans-Peter Dumm for always asking, "Why?" He forced me to learn so much when I would discuss aspects of my research with him and he would simply ask, "Why is that so?" or, "Why is that happening?" It allowed me to really think critically and not forget what I already know.

To Dr. Rafiqul Tarefder, my advisor and committee member, for your valuable input to this research and making sure I knew what I was doing in ABAQUS CAE.

And finally, a huge thanks to everyone in my family. With everyone's love and support I couldn't have survived through a single day of graduate school. Love and support is surely one thing that I will always have copious amounts of from everyone in my family.

Thank you all for everything.

THE DEVELOPMENT OF A MODIFIED BI-AXIAL COMPOSITE TEST SPECIMEN

BY

ANTHONY SAMUEL TORRES

ABSTRACT OF THESIS

Submitted in Partial Fulfillment of the
Requirements for the Degree of

Masters of Science
Civil Engineering

The University of New Mexico
Albuquerque, New Mexico

May, 2010

THE DEVELOPMENT OF A MODIFIED BI-AXIAL COMPOSITE TEST SPECIMEN

by

ANTHONY SAMUEL TORRES
B.S., Civil Engineering, New Mexico State University, 2008
M.S., Civil Engineering, University of New Mexico, 2010

ABSTRACT

Bi-axial testing of composite structures has been an important topic in the research community for some years now. Bi-axial test specimens in the past have typically been cruciform specimens with a tapered thickness gage section. This ensures that the specimen will fail under bi-axial loading rather than uni-axial loading due to high stress concentrations at the intersecting loading arms. To reduce the stress concentration in the loading arms the intersection points are rounded and curved inward toward the center of the specimen. By having the curvature of the intersecting arms come closer into the specimen it reduces the amount of uni-axial stress at that point. In order to reduce the stress even more, tapered thickness gage section milling is required to achieve adequate bi-axial failure. In the proposed research these specimens will be modified so that no milling of the gage section is required. The process of milling the gage section of the composite laminate could inflict initial damage to the specimen which would yield inaccurate results. The modified bi-axial specimen will instead have aluminum shims bonded to the rounded corner to ensure bi-axial failure. The location of the shims was determined using Finite Element Analyses which verified the location and magnitude of the stress concentrations. The use of the aluminum shims could allow the cruciform specimen to be completely unscathed of any initial damage.

The specimens are thick woven carbon fiber/epoxy bi-axial specimens which previously haven't been tested before. Two types of geometries were fabricated, one out of IM7/UF3352 and one out of IM7/PATZ materials, both with a [(0/90)]s lay-up. The first geometry had the aluminum shims. The second configuration consisted of a smaller composite laminate sandwiched in between two pre-fabricated G10 glass/epoxy panels and only machining away the G10 material, keeping the composite laminate unscathed. Both geometries had tapered thickness gage section counterparts for comparison purposes. The shimmed design showed undesirable failure modes but provided a reliable lower bound for bi-axial strength design. The sandwich panel design showed ideal failure conditions for all tests. This shows that a modified bi-axial composite specimen can be developed that limits the amount of machining and can still produce accurate results.

Additional tests were conducted to study the effect of stress concentrations around holes of different diameter under biaxial load. Results were interpreted with the aid of Finite Element Analyses.

TABLE OF CONTENTS

LIST OF FIGURES

LIST OF TABLES

Section 1

INTRODUCTION

1.1 PURPOSE OF PAPER

The overall purpose of this research was to develop a cruciform bi-axial composite specimen that has as little initial damage, caused by machining, as possible. The significance of bi-axial testing is to generate experimental failure data, which can be used to validate numerous failure prediction models [1]. Existing failure theories have not been proven to be accurate for predicting failure for laminated composites [1]. Eighteen woven carbon-fiber cruciform specimens were made for bi-axial testing, six of which limit the amount of machining on the specimen. The remaining twelve cruciform specimens were used for comparison purposes and an additional test on the effect of stress concentrations around a hole in the center of a cruciform specimen.

1.2 OVERVIEW OF RESEARCH

Typical cruciform specimens have a tapered thickness gage section that allows bi-axial failure to occur, known as a standard cruciform specimen [1]. The gage section is defined as the center of the intersecting loading arms in the cruciform specimen, where bi-axial stress occurs [1]. The purpose of the tapered thickness gage section is to increase the amount of bi-axial stress and force failure to occur in the gage section. If the cruciform specimen fails outside the gage section then it is not failing under a bi-axial stressed state. The tapered thickness gage section is typically milled with a high speed mill and router to a depth of 25% the thickness on each side of the composite. In this

study, no machining of the gage section was done on the newly developed specimens. Instead, aluminum shims were adhered to the specimen in an attempt to minimize the highly stressed areas outside of the gage section, thus leading to bi-axial failure. In addition, the specimens were fabricated out of a woven composite material as well as being uncharacteristically thick. Specimens in the past have had a maximum thickness of 0.20 inches. Specimens tested in this research have an average thickness of 0.25 inches.

Three sets of tests were completed in this research, each set having a standard tapered thickness cruciform used as a control specimen for comparison. The initial set of tests using, shimmed cruciforms and standard tapered thickness cruciforms, will be denoted Type I tests. The second set of tests using built-up cruciforms and standard tapered thickness cruciforms will be denoted Type II tests. The built-up cruciforms consist of a thinner woven carbon-fiber laminate sandwiched in between two pre-fabricated G10 glass-epoxy plates. The specimens have a tapered thickness gage section but only the G10 material is machined away. This left the woven carbon-fiber laminate unscathed. Both specimens have a different geometry from the Type I tests. The change in geometry is discussed in Section 4.6. The last set of tests using shimmed cruciforms with a center hole and a standard tapered thickness cruciform with a center hole, will be denoted Type III tests. Type III tests use the same geometry as the Type I tests but with a ¼" hole in the center. All three tests have identical standard tapered thickness specimens. These specimens will be denoted control specimens.

1.2 INTRODUCTION

One of the main advantages of bi-axial testing is that it allows a more accurate material characterization. Simply limiting material evaluation to uni-axial testing can lead to an inaccurate representation of the material. Therefore, engineers may have to use an overly conservative design to ensure the structure does not fail. Composite materials, like carbon fiber reinforced epoxy, have the potential to greatly lighten aerospace structures due to their high specific stiffness. Over designing the structure ultimately hinders the potential of the material. The loading on aerospace structures is typically multi-axial, therefore using more realistic loading conditions in the lab can lead to a better representation of the structure when it's in use. An accurate material characterization can establish a way forward to the next generation of advanced structures.

In addition, aerospace structures are typically fabricated out of fiber reinforced polymers such as carbon-epoxy and glass-epoxy composite materials. Typical specimens are thin with thicknesses up to 0.2 inches. Also, the composites are usually made from uni-directional plies, also known as tape composites. Unidirectional means that the fibers in an individual ply of the composite lay-up run in a single direction. This is in contrast to woven materials, which have one or more tows going different directions in the same ply. Therefore, previous research in the bi-axial community has been limited to cruciform specimens that have thin, uni-directional, composite components. Figure 1.1 shows a typical cruciform specimen used for bi-axial testing.

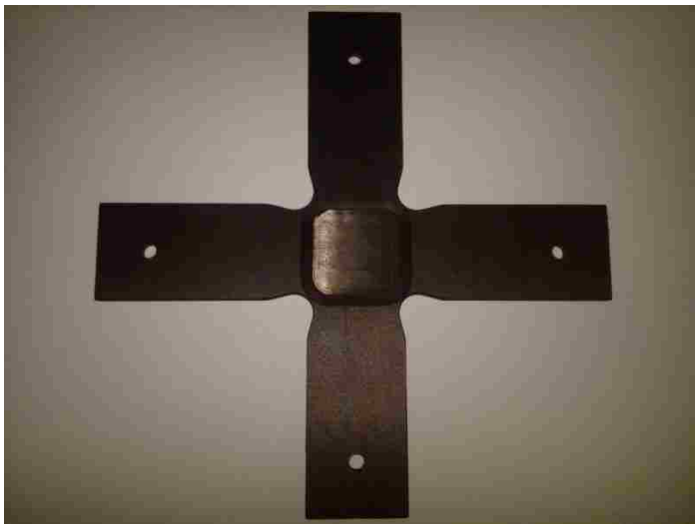

Figure 1.1: Typical thin uni-directional bi-axial cruciform specimen [1].

A structure that is in a bi-axial stressed state could also have a bolted connection directly through the bi-axial loaded zone. An example of this is a pressure vessel. The internal pressure on opposing walls induces the bi-axial stress state while the bolts are often used to attach connecting plumbing or simply to hold the pressure vessel caps in place. The addition of the hole for the bolt will cause a stress concentration that could lead to failure. Accurately characterizing failure under this particular instance is important. The addition of the whole in the center of the gage area could significantly reduce the strength of the cruciform specimens, in turn causing a catastrophic failure. Failure due to a stress concentration around a hole has previously been tested in a uni-directional specimen but not in woven carbon-fiber cruciform specimens. These tests will provide data showing the percentage of load the specimens can withstand in the presence of a hole under a bi-axial stress state. Tension testing of this scenario is more significant than a compression test because we have assumed that the hole will be filled with a bolt or connector.

1.3 OUTLINE OF PAPER

The main purpose of this study is to develop a new cruciform specimen with minimal initial damage. The new specimen will make use of aluminum shims to reduce the high uni-axial stress in the arms as opposed to milling the center of the specimen. The new specimens are also thicker than typical cruciform specimens and are fabricated out of a woven carbon fiber composite material. To the author's knowledge, bi-axial testing on woven composites has not been done before. Section 2 discusses related work in the bi-axial testing community including information on the tri-axial test facility, located at the Air Force Research Laboratory (AFRL) Space Vehicles Directorate. This facility was used for this research. This is followed by a section on the experimental procedures used to design, fabricate, and test the modified bi-axial test specimen. Section 4 contains the results from the tests as well as a discussion on the outcome of the new design. Included in the discussions are recommendations for improvements of this design. The final section wraps up the research with a conclusion and a discussion of further improvements.

Section 2

BACKGROUND INFORMATION AND LITERATURE REVIEW

2.1 INTRODUCTION

This section reviews background information on bi-axial loaded composites. A discussion on the different biaxial test methods is presented. Also discussed are the developments in biaxial testing and improvements on the cruciform specimens done by other researchers. Lastly, this section includes information on the biaxial facility located at the AFRL.

2.2 BIAXIAL TEST METHODS

There are different methods that have been used for testing composites under biaxial loading [2]. The types of tests have been placed into two main categories; i) those that use a single loading system which generate biaxial stress from the unique geometry of the specimen, and ii) those that use two or more orthogonal loading systems to achieve biaxial stress. The first method is simpler because a conventional test machine can be used. The key disadvantage is that the stress field may not be uniform due to the geometry of the specimen. The second method uses two actuators to keep the specimen centered and is more typical.

The first method can be done using tubular specimens as described by Swanson [3]. Swanson describes what is called the "free-edge effect" in composites. The effect refers to the stress concentration that occurs at the edge of a laminate due to the mismatch of the individual ply properties. The use of tubular specimens overcomes this edge effect

problem as well as achieving biaxial loading. The bi-axial loading on the tubular specimen involves a combination of hoop stress and axial tension/compression stress. The specimen is fitted with a rubber bladder that is pressurized with a silicone oil to create the hoop stress and a servo controlled universal testing machine is used for the axial tension/compression stress. Loads are applied and the ratio of the axial to hoop stress can be adjusted. The servocontrol is used to control the ratio of the axial to hoop loading, with the internal pressure applied independently and the axial load slaved to the output of the pressure transducer.

The second method can be done using a tabbed cruciform specimen as described by Ash and Welsh [1]. Ash and Welsh generated accurate biaxial failure data for laminated fiber-reinforced materials. The specimen fabrication process involves laying-up a flat laminate plate with the desired lay-up combination. The cruciform geometry and gage section is machined using a computer numeric controlled (CNC) mill and router. The gage section of the cruciform specimen is described as a reduction in thickness directly in the center of the cruciform; this is done where failure is desired. It is believed, by Ash and Welsh, that there is a possibility of fiber damage created when the gage section is machined out and a new lay-up method can be developed to eliminate this initial damage [1]. The new cruciform lay-up that Ash presented involved preparing a thinner carbon fiber laminate and sandwiching it between two glass fiber tabs with the same geometry. The two outside sandwich panels contain the machined gage section. The specimens are referred to as “built-up specimens” [1]. Failure for these new specimens occurred in the narrow section of the arms thus leading to undesirable failure mode. Testing also included the standard tapered thickness specimens for comparison.

Scatter in the results showed that the built-up cruciform specimen was not conclusively better than the control specimens. Overall, the test on built-up specimens confirmed that the initial damage due to machining the gage section is not very significant. Although undesirable failure modes were shown, the author believes that improvements can be made to this design to achieve adequate failure modes. Type II tests specimens will be very similar to these specimens, the differences are discussed in Section 4.

2.3 IMPROVEMENTS IN BI-AXIAL TESTING

Hemelrijk et al. [4] describes the development of biaxial cruciform specimens as well as comparing two different methods for monitoring deformations during loading. Four different geometries were modeled in a finite element program. The geometries can be seen below.

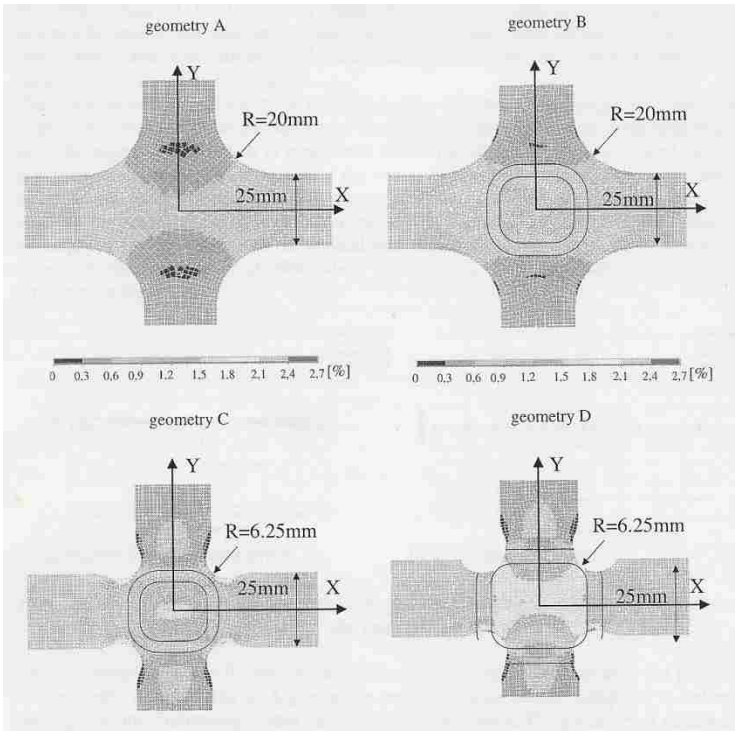

Figure 2.1: Shows the four geometries developed by Hemelrijk et al [4].

These geometries all use rounding at the corner of the intersecting load arms to reduce stress in the corners. The FEA showed that geometry C and D contain higher values of biaxial stress in the gage section. Therefore, geometries C and D were tested in a biaxial testing machine. The specimens were instrumented with strain gages and Digital Image Correlation (DIC) was used to measure strain over a large area. DIC is a technique used to determine displacement and deformation fields at the surface of objects based on a comparison between images taken at different load steps. Overall, the results showed that the strain read from the strain gages are extremely close to that of the DIC. In addition to the developments on the cruciform geometry, this study shows how the use of DIC can be used in place of the typical strain gages.

Welsh and Adams [5] present a study that includes the effects of triaxial loading conditions. The main hypothesis of this study is that a thickness-tapered cruciform specimen can be used to perform both biaxial and triaxial tests by applying through thickness forces perpendicular to the gage section. Although this article mainly discusses triaxial loading, it also discusses improvement to the cruciform specimen design. One of the improvements was the elimination of one of the wedge grip alignment holes. Wedge grips are used to apply the load to the cruciform arms. Previously two small holes had been drilled into each arm to align the wedge grips. The second hole was removed because the uniaxial stress in each loading arm increases to the maximum value at the inward edge of the wedge grip. Thus removing the second hole minimizes the possibility of undesirable failures to occur in the loading arms [5].

Additional research by Welsh and Adams showed how changes to the geometry of the tapered cruciform specimen affected the measured biaxial strength of composites

[6]. Another modification that was done was to increase the width of each arm of the cruciform to 1.25 inches, which is the capacity of the test fixture. This change lowers the uniaxial stress state in each loading arm, which also minimizes any undesirable failures in the arms. Two additional changes were made, one being the radius of the corner that joins two intersecting loading arms. The second being the actual shape of the gage section. Two types of tapered gage sections were tested to determine the effect of the tapered gage section shape. Round and square shaped gage sections were investigated. The stress in the gage section was calculated using strain data from a strain gage and stiffness data from uni-axial tests. Due to the cruciform geometry of the specimens, the stress in the gage section is not the same as the stress applied to the arms [1,6]. This is due to a portion of the load being reacted by the transverse arms [1,6]. The actual stress in the gage section is determined by multiplying the strain from the strain gage by the modulus of the material. A Bypass Correction Factor (BCF) can be used to determine the stress in the gage section in additional specimens that do not have strain gages [1,6]. The BCF calculation can be seen in the below equation.

$$BCF = \frac{(Modulus)_{effectiv}\varepsilon_{measured}}{(Load)_{measured}/(Area)_{Measured}} \quad \text{Eq. 2.1}$$

The BCF is used to determine the stress in the gage section in non-strain gaged specimens. Welsh and Adams showed that the small rounded gage section received 21% of the load and the square gage section received 70% of the load. It was determined that the small square gage section was the optimum configuration for this study. This is due to the square gage section receiving more of the load than the rounded gage section. A schematic of the types of gage sections discussed in this study can be seen in Figure 2.2.

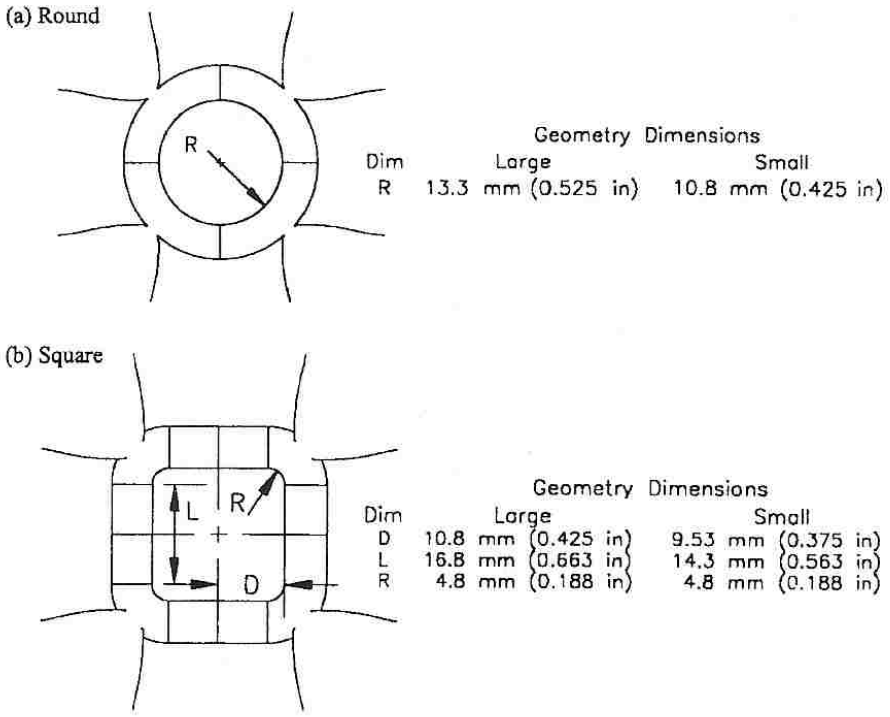

Fig. 5. Round and square gage section details for the thickness-tapered cruciform test specimens.

Figure 2.2: Cruciform gage section geometry developed Welsh and Adams [6].

This study showed that changes to the cruciform geometry improved the likelihood of bi-axial failure.

2.4 BI-AXIAL AND TRI-AXIAL TEST FACILITY AT AFRL

The article by Welsh and Mayes [7] describes the triaxial test facility at the Air Force Research Laboratory Space Vehicles Directorate. The triaxial test facility is capable of generating any combination of tensile or compressive σ11, σ22, and σ33 stresses. It has a capacity of plus or minus 133kN on each of the 6 computer controlled actuators and is limited to quasi-static test rates. To ensure that the facility was running properly biaxial tests were run on the machine for validation purposes. The biaxial tests

were done on standard tapered thickness gage section composite laminates as presented in previous biaxial testing. The experimental failure data was compared to data obtained from Multi Continuum Theory (MCT). Overall, the close correlation of MCT's analytically generated failure envelopes with the experimentally generated failure envelopes validate the experimental method.

2.5 CRUCIFORM SPECIMENS WITH CENTER HOLES

Isaac Daniel describes the behavior of graphite/epoxy composites with holes while under bi-axial loading [8]. Multiple quasi-isotropic composite plates with varying hole sizes were tested under bi-axial loading to investigate the influence of hole diameter on failure. Four diameter holes were tested: 1 in., 0.75 in, 0.50 in and 0.25 in. Bi-axial loading was induced by the use of four whiffle-tree grip linkages and controlled with a servo hydraulic system. The deformations and stresses around the holes were measured using strain gages and birefringent coatings. The specimens were from SP-286T300 8-ply [(0/45)(-45/90)]s 16 in. x 16 in. plates. The plates were tabbed with 5-ply crossply glass-epoxy tabs with a circular cutout leaving a gage area in the center. The tabbing material is placed over the square plate to create the cruciform specimen. The gage area contained a center drilled hole with varying diameters. The test showed that at high loads birefringence concentration appears at angles of 22.5˚ off the horizontal and vertical axes. Cracking and delamination initiates at these zones. The stress at these zones reached up to twice that of the stress of a specimen without a hole. Birefringent coatings will not be used in my experiment.

D.L Jones [9] has completed other research on bi-axial specimens containing center holes. The main focus of this study was to determine the effect of bi-axial loads and fatigue testing on the same composite specimen. The study also included a residual strength test on a cruciform containing a center hole. Different test parameters consisted of changes in load, hole diameter, and the laminate lay-up. The tests were conducted on a test frame with horizontal and vertical servohydraulic actuators. Due to the use of the separate actuators the test configuration could not keep the center of the specimen stationary. Therefore, the horizontal axis was suspended by elastic ropes to prevent any side loading. The cruciform specimen was approximately 12 in. by 12 in. with a 3 in. by 3 in. area cut from each corner, which gave it the cruciform shape. The specimen did not have a milled gage section. The specimen consisted of a eight and sixteen ply laminate ($[(0/45)(-45/0)]_{2s}$ and $[(0/45)(-45/0)]_{4s}$) made from Thornel 300/Narmco 5208 graphite-epoxy. Hole diameters of 0.5 in, 1 in, and 2 in were tested. The tests showed that the hole diameter had a limited influence on the static strength, when the strength was based on the net area. However, they state that not enough specimens were tested to make this a definitive conclusion. The main differences from this research are the shape of the cruciform specimen, the test set-up, and the inclusion of the fatigue loading. Had the authors chose to use the gross area in their analysis rather than the net area it would have showed the failure stress to be less than that of the none hole specimen. By using the net area they are not comparing the same failure strength to each other. The ultimate goal of their study was to see if the specimen could take the same amount of load across the entire bi-axial loaded region having a hole drilled directly through it. This seemed possible to the researchers due to the large gage section.

2.6 CONCLUSIONS

Due to the authors indication that machining may be influencing the measured biaxial strength the author chose to develop a new bi-axial test specimen that doesn't require a machined gage section. Aluminum shims will be added to the high stress zones to force failure in the biaxial loaded region. Strain gages will be used to obtain ultimate stress data by multiplying the measures strain by the modulus of the material. Due to undesired failure in the arms of the Type I specimens, a built-up specimen was added to this research. The built up specimens tests are denoted Type II tests in accordance with the specimen type. Along with the built-up panel addition, specimens with a center hole were also investigated. These tests are denoted Type III tests. The procedures and results are shown in the next two sections.

Section 3

EXPERIMENTAL PROCEDURES

3.1 INTRODUCTION

This section starts with a description of the Type I cruciform design. This is followed by a discussion of how the final cruciform design was fabricated. Tensile properties, density, and fiber volume content tests were completed to better understand the material. A description of the bi-axial testing, including sample preparation, test equipment, and test procedures are in the following section. The material used for this experiment is IM7/UF3352 (TCR Composites, Ogden, Utah) and IM7/PATZ (PATZ Materials Technology, Benicia, California) with G10 glass-epoxy panels (Ridout Plastics Co, San Diego, California). All material properties are in Appendix A. All fabrication and testing was done by the author with assistance from employees of the Air Force Research Laboratory (AFRL) Space Vehicles Directorate.

3.2 BI-AXIAL SPECIMEN DESIGN

The cruciform shape was based on the bi-axial cruciform design in Ref. 6. The changes made to the specimen are the total length of the specimen (6.34 instead of 6 in.), the width of the arms (1.2 instead of 1 in.), and the amount the rounding of the intersecting arms are separated by (.85 in. instead of .76 in). The geometry was compatible with the fixtures in the tri-axial test frame. The design used circles to form the inner rounding of the intersection arms, as shown in Figure 3.1.

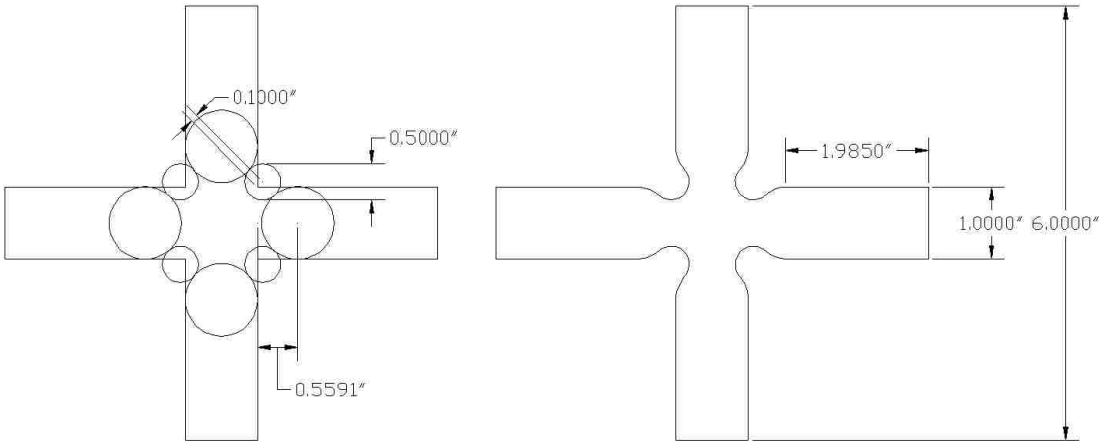

Figure 3.1: Schematic drawing of the cruciform geometry.

The purpose of rounding the intersecting corners was to decrease the uni-axial stress concentration at the corner of the intersection load arms and transfer it to the center of the cruciform. Stress analysis shows that the geometry alone is not sufficient to yield bi-axial failure. Gage section milling or additional shims are required. This effect can be seen in Figure 3.2. Symmetrical geometry was used in the FEM to reduce errors.

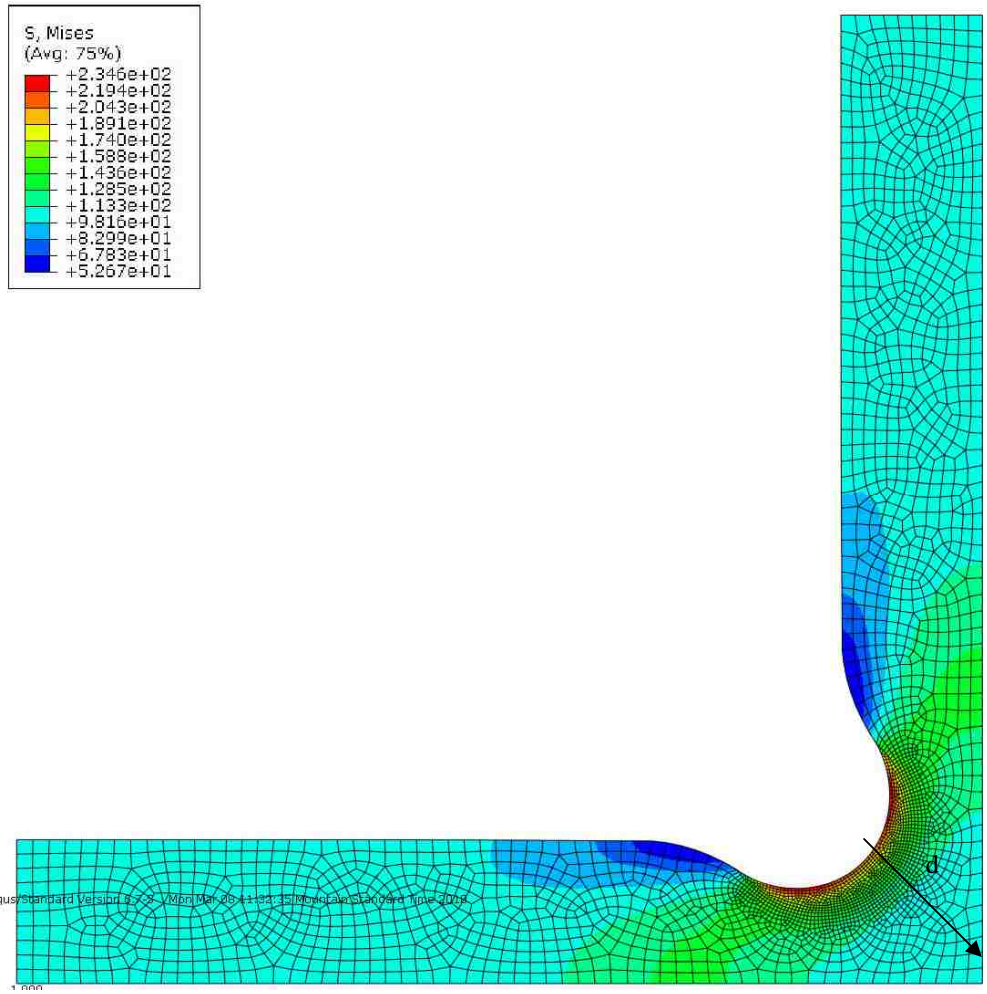

Figure 3.2: Distribution of von Mises stress in a 1/8 symmetrical model analyzed in ABAQUS.

A mesh refinement convergence test was done on the rounded corner of the specimen to check for accurate stress simulation. A close up of the rounded corner with the refined mesh can be seen in Figure 3.3. The graph of stress vs mesh size for elements at the corner is shown in Figure 3.4. The graph plots the stress along line d shown in Figure 3.2. The mesh size was then manually refined by half the size and the maximum stress value was recorded again. This process was repeated until the stress value converged at a value of 234 ksi. The stress converged at an element size of .002 in.

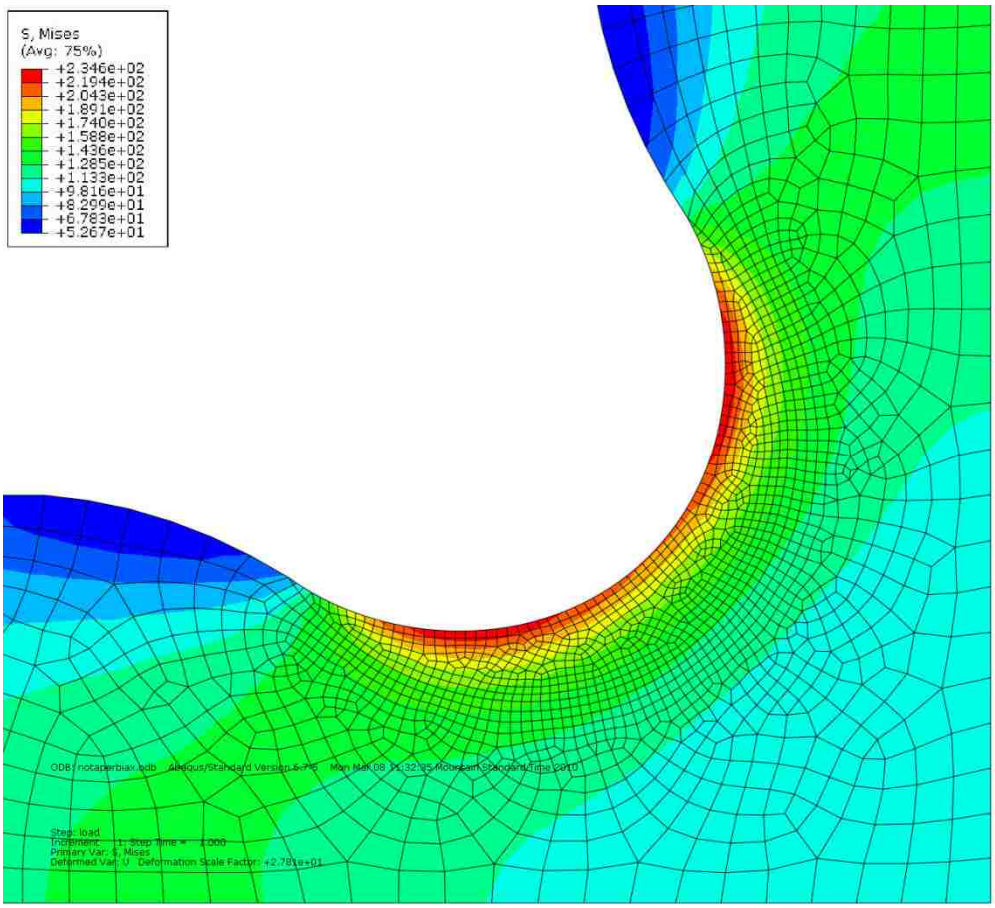

Figure 3.3: Mesh refinement at rounded corner.

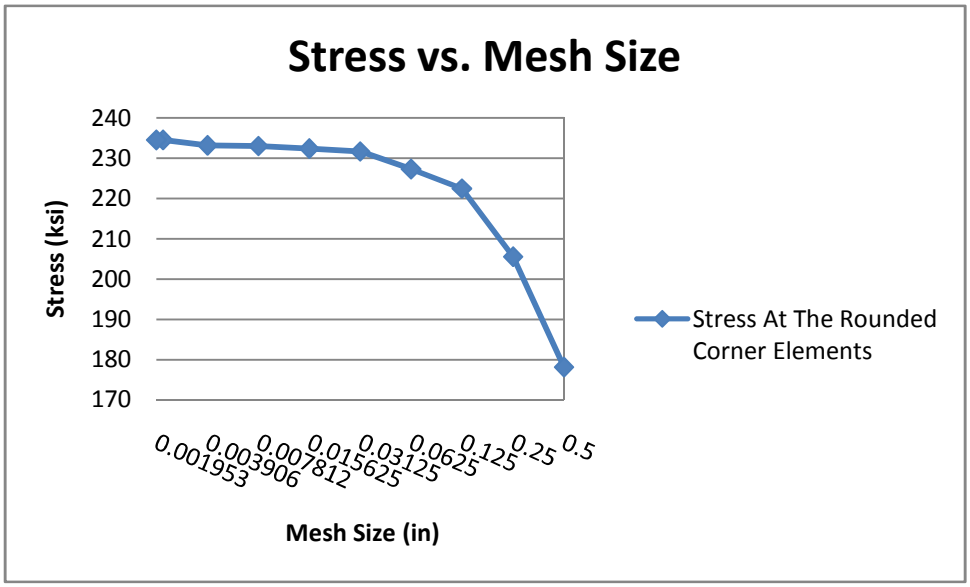

Figure 3.4: Stress convergence vs. Mesh size at the rounded corner.

A 1/1 load ratio, same amount of load applied in the x direction as in the y, was applied to the model and the resultant von Mises stress is shown in Figure 3.2. The von Mises stress plot shows a high stress area at the rounded corner of the cruciform. The maximum stress shown has a value of 234 ksi from an applied stress of 100 ksi. As stated previously, if the cruciform specimen is not failing in the gage section it is not failing under bi-axial loading [1]. Thus, the FEM for the cruciform should show a high stressed area in the gage section, instead of being just at the rounded corner. Therefore, to reduce the stress at the rounded corner aluminum shims were added to the cruciform specimen. A crescent moon shaped aluminum shim was adhered to both faces of the specimen at each rounded corner. The interface of the shim and composite was modeled with a tie constraint. The tie constraint permitted the two parts to act as one uniform element. FEM showed a decrease in stress at the rounded corner due to the addition of the shim.

Although, the abrupt change in thickness caused a stress concentration at the cusp of the shim, as shown in Figure 3.5.

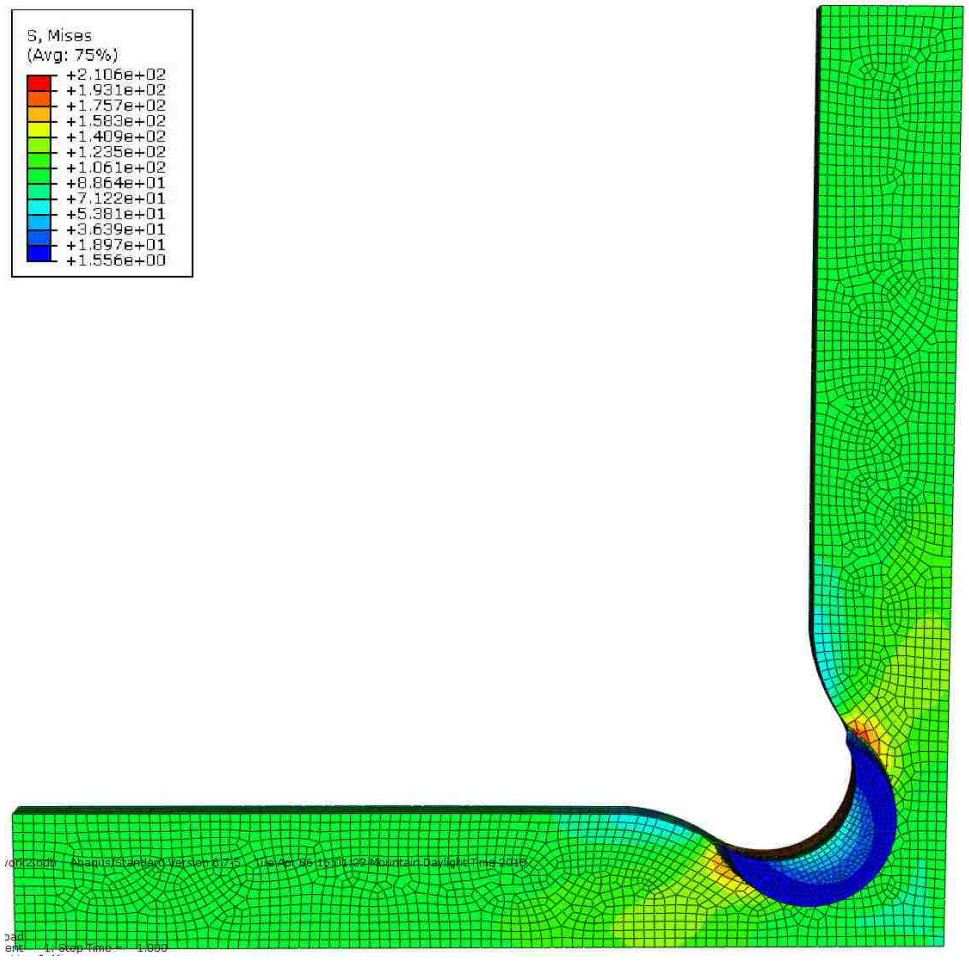

Figure 3.5: Analysis showing the addition of the aluminum shims and the associated decrease in stress levels at the rounded corner compared to the non-shimmed control specimen.

Although the addition of the shim caused a stress concentration, the shim design was still tested, the results are described in Section 4. The shims were optimized to cover the high stress at the rounded corner using the FEM stress plot shown in Figure 3.2. Due to the cruciform geometry not having a tapered thickness gage section, the area at which

the elements have the same stress in each direction is more difficult to define. The area at which this occurs was determined by recording the two principle stresses for each element from the middle of the rounded corner to the, bottom right corner, center of the cruciform. Once the two opposing stresses were within 5% of each other is where the gage section was defined for this particular cruciform. The shim length was designed to cover from the rounded corner up to the point of the bi-axial stressed elements. The thickness of the shim was determined by mechanics of materials and the equilibrium of forces on the cruciform. The equilibrium of forces can be represented by their stress counterparts shown in EQ 3.1.

$$\sigma_{corner} t_{comp} = \sigma_{applied} t_{comp} + \sigma_{al} t_{shim} \quad \text{EQ 3.1}$$

Where σ_{corner} is the amount of stress at the rounded corner. t_{comp} is the thickness of the composite. $\sigma_{applied}$ is the amount of stress applied to the composite. σ_{al} is the amount of stress in the aluminum shim and t_{shim} is the thickness of the shim.

EQ 3.1 can be re-written to solve for the thickness of the shim, as follows:

$$t_{shim} = \frac{(\sigma_{corner} - \sigma_{applied}) t_{comp}}{\sigma_{al}} \quad \text{EQ 3.2}$$

By definition:

$$S.C. = \frac{\sigma_{corner}}{\sigma_{applied}} \quad \text{EQ 3.3}$$

Where S.C. is the stress concentration. Plugging EQ 3.3 into EQ 3.2 gives us the following equation:

$$t_{shim} = \frac{(\sigma_{applied S.C.} - \sigma_{applied})t_c}{\sigma_{al}} \quad \text{EQ 3.4}$$

Simplifying EQ 3.4:

$$t_{shim} = \frac{\sigma_{applied}}{\sigma_{al}} t_c(S.C. - 1) \quad \text{EQ 3.5}$$

Since the strain in the aluminum is the same as in the composite the stress can be represented by the moduli of each material, giving the final equation.

$$t_{shim} = \frac{E_c}{E_{al}} t_c(S.C. - 1) \quad \text{EQ 3.6}$$

Where, E_c is the modulus of the composite and E_{al} is the modulus of the aluminum shim.

The aluminum shim design was tested in the bi-axial load frame located at AFRL with a 1/1 load ratio. The results were then compared to the cruciform specimens with the tapered thickness gage section.

3.3 SPECIMEN FABRICATION

This section describes the fabrication of the control and the shimmed bi-axial cruciform specimens.

3.3.1 COMPOSITE LAY-UP

The shimmed specimens used IM7/UF3352 carbon-epoxy satin weave (four-harness) fabric. The four-harness indicates a satin weave which has tows in the 0 and 90 degree directions like a plain weave, but each tow goes over 3 perpendicular tows and then under 1. Two different layups were investigated. The first lay-up was a $[(0/90)_8]_s$ and the second layup was a quasi-isotropic

$[(0/90)_4(45/-45)_4]_s$. The material was cut to 14 in. x 18 in. The plies were cut on a GERBERcutter CNC machine.

The lay-up process was done by hand in a jig for corner alignment, as seen in Figure 3.6.

Figure 3.6: Lay-up process with aluminum jig for corner alignment.

The layup was debulked after every two plies using a BriskHeat vacuum and curing table (BriskHeat, Columbus, Ohio). Debulking was done with a vacuum of 10 psi and a temperature of 85 deg F.

Once the plies had been stacked in twos, the process was continued by stacking each of the debulked plies together, and repeating until the final lay-up is achieved. Once the plate was completely debulked and layed-up then it was placed in an autoclave and cured to the manufacturer's specification.

The finished plates can be seen in Figure 3.7.

Figure 3.7: Completed IM7/UF3352 plates.

3.4 SPECIMEN MACHINING

The specimens were machined according to the schematic in Figure 3.1. Uni-axial specimens were machined from the same plate for material characterization.

3.5 BI-AXIAL CRUCIFORM SPECIMENS

For the Type I tests, half of the specimens were fitted with the aluminum shims and the other half were machined so that they had a tapered thickness gage section. The specimens with the tapered thickness gage section were the control specimens. The shims were bonded to the specimens with Hysol 9309 epoxy adhesive (Henkel Corperation, Bay Point, California). The shimmed specimens were then cured in an oven for 6 hr at 185˚F. Pictures of the control and shimmed specimens can be seen in Figure 3.8 and 3.9 respectively.

Figure 3.8: Control specimen.

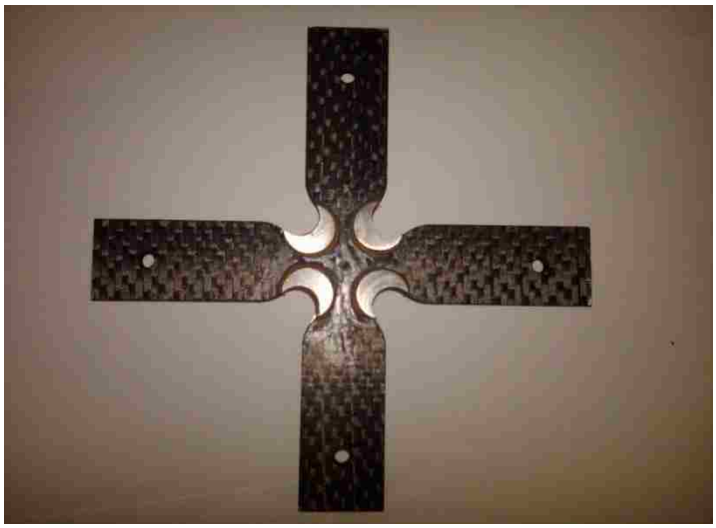

Figure 3.9: Shimmed specimen.

3.6 MATERIAL CHARACTERIZATION

The IM7/UF3552 material's ultimate strength, modulus of elasticity, and Poisson's ratio were measured using a uni-axial tension test. The fiber content and

density were also measured. The IM7/PATZ material was not characterized. The PATZ resin is analogous to 977-2 resin, therefore 977-2 values from Ref 1 were used when necessary.

3.6.1 UNI-AXIAL TENSION TEST

The tension tests followed a modified ASTM D3039-07 "Standard Test Method for Tensile Properties of Polymer Matrix Composite Materials" [10]. Eight uni-axial test specimens were tension tested (four of each lay-up) two of which were tested October 20, 2009. The remaining six were tested February 2, 2010. All testing was conducted at the AFRL. The only variations from the standard was the thickness of the specimen which was 0.25 inches as opposed to the recommended 0.1 inches. The material used for this experiment was the IM7/UF3352 with two different lay-up configurations: $[(0/90)_8]_s$ and $[(0/90)_4(45/-45)_4]s$. The $[(0/90)_8]_s$ specimens were the first two tested in February. The fabrication process is shown in Section 3.3.1 and was done in August 2009. The average ply-thickness for this material is 0.008 in. The specimens were machined using a high speed mill and router at the University of New Mexico Mechanical Engineering machine shop (UNM ME). The specimens had a rectangular geometry having the following dimensions: 10 in. x 1 in. x 0.25 in. The last six specimens tested were tabbed with G10 glass-epoxy tabs and Hysol 9309 epoxy adhesive. They were each labeled with a 90 or a 45 to designate the lay-up configuration. The 90 referred to the $[(0/90)_8]_s$ and the 45 referred to the $[(0/90)_4(45/-45)_4]s$ lay-up. These numbers were then followed by the number 1 through 4, to designate the test number. The tensile testing was done on an Axial-

Torsional Material Test System (MTS, Eden Prairie, Maine) with hydraulic wedge grips with a displacement rate of 0.05 in. per second. Specimens were instrumented with bi-axial strain gages, one for axial and one for transverse strains. The strain gages were CEA-00-125UT-350 (Vishay, Malvern, Pennsylvania). The measured strains were used to calculate the Poisson's ratio and the modulus of elasticity.

3.6.2 DENSITY AND FIBER VOLUME CONTENT

Fiber volume was determined according to ASTM D3171-06, "Standard Test Methods for Constituent Content of Composite Materials" [11] using Procedure G: Matrix Burnoff in a Muffle Furnace. The material used was IM7/UF3352 with the dimensions of: 0.25in x 0.25 in x 0.25 in. The fiber density values used can be seen in Table 3.1 below.

Table 3.1: Values used to calculate results for Density, Fiber Volume, and Void Volume [12].

Water Temp (deg C):	16.5
Water Density (g/cc):	0.99886337
Resin Density (g/cc):	1.208
Fiber Density (g/cc):	1.795

The specimens were placed in a muffle furnace for a period of 14 hours at a temperature of 835 degrees Fahrenheit.

3.7 BI-AXIAL TESTING

All bi-axial testing was done by Adam Biskner and Anthony Torres at the AFRL from February 11, 2010 – March 18, 2010. The materials tested were IM7/UF3352 and IM7/PATZ with G10 glass-epoxy. The lay-up configurations for the IM7/UF3352 material is $[(0/90)_8]_s$ and for the IM7/PATZ are $[(0/90)_2]_s$ and $[(0/90)_3]_s$. The average ply thickness for both materials is 0.008 in. The IM7/UF3352 specimens were machined at the UNM ME machine shop and the IM7/PATZ specimens were machined at the AFRL. Twelve specimens were tested from the IM7/UF3352 material and six specimens were tested from the IM7/PATZ material. Six of the first material had aluminum shims glued on with Hysol 9309 epoxy adhesive while three of the second material had G10 glass-epoxy material glued with the same adhesive. A displacement rate of 0.05 in per second was used for all tests. Two types of strain gages were used, CEA-06-125UW-360 and CEA-00-125UT-350. The uni-axial strain gages were used with the Type I shimmed specimens due to the lack of room for a bi-axial strain gage. Instead two uni-axial strain gages were used, one on each side in opposing directions. The test equipment and test procedure can be seeing in the below sections.

3.7.1 TEST EQUIPMENT

The tri-axial test machine located at the AFRL [13] was used for biaxial tests. A picture of the machine can be seen in Figure 3.10.

Figure 3.10: Tri-axial test machine.

Although this machine is capable of testing in three orthogonal directions simultaneously, only the x and y directions were used.

The machine works by holding the each arm of the specimen in wedge grips. The wedge grips are housed by arm fixtures. The arm fixtures are attached to four screw driven actuators that can apply tension or compression in two orthogonal directions. The actuators are displacement controlled and the applied load is measured using load cells.

3.7.2 TEST PROCEDURE

There is no published ASTM standard for a cruciform bi-axial test. The procedure used is as follows:

1. Using the appropriate wedge grip arms (compression/tension). Place on elevated blocks and unscrew the arm covers.

2. Obtain appropriate wedge grips for specific thickness bi-axial specimens and place in alignment holes as shown in Figure 3.11

Figure 3.11: Placement of wedge grip in alignment hole on specimen.

3. Place specimen with wedge grips in arm fixture. See Figure 3.12.

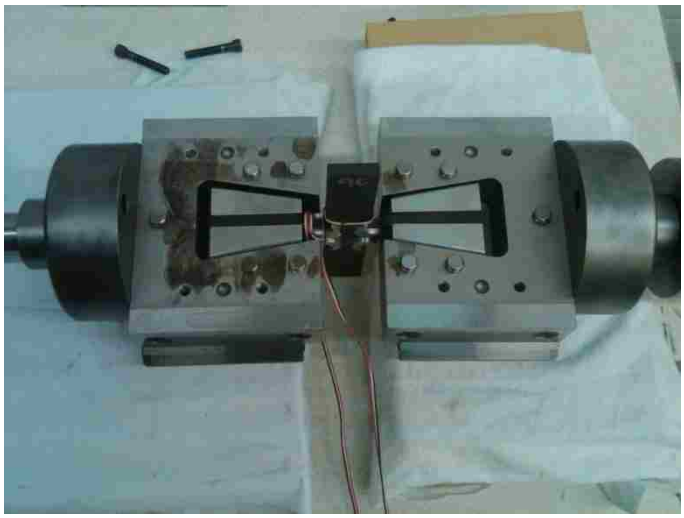

Figure 3.12: Specimen and wedge grips placed in the wedge grip arms.

4. Place the provided spring in an "L" shape in the center of all of the wedge grip arms to prevent any sliding.

5. Now the angled bearings can be placed on top of the wedge grip arms and the final assembly should look like that of Figure 3.13.

Figure 3.13: Correct placement of all wedge grip arms, spring, and bearings.

6. Before running the test the signal conditioners were balanced for both the load and the strain.
7. Once all signal conditioners had been calibrated to specified inputs (provided in text document attached to computer) then open triax program on computer.
8. Attach arm fixtures to actuators shown in Figure 3.14.

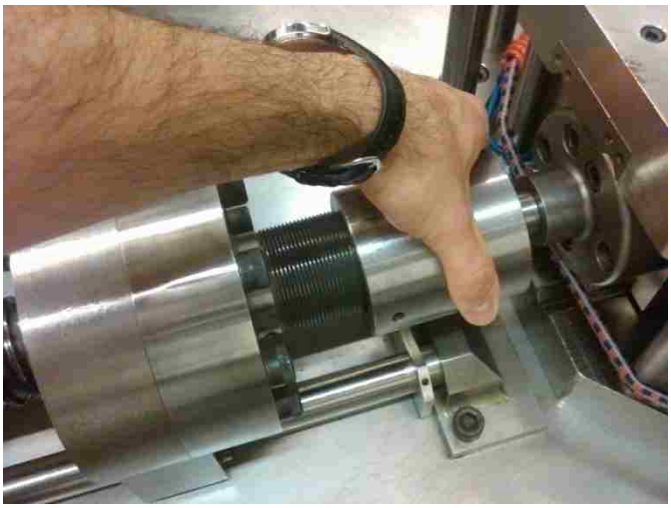

Figure 3.14: Tightening the cylindrical housing from the wedge grip arms to the screw drive.

9. Now that the fixture is fully attached to the machine go into the "Pre-Load" menu and ensure that a small initial load of 5-10 lbs is balanced between all arms.
10. Run test.

3.7.3: STRESS CALCULATIONS

Due to the cruciform geometry of the specimens and the gage section in some specimens having a reduced thickness, the stress in the gage section is not the same as the stress applied to the arms [1]. A Bypass Correction Factor (BCF) which relates the applied stress to the stress in the gage section (Eq. 3.2) was therefore used to accurately determine the stress in the gage section [1]. While the stress in the gage section can be accurately determined from the strain gage data (multiplied by the elastic modulus) while the material is elastic, it is not feasible to do this beyond the elastic range of material behavior.

The BCF was determined using the following steps:

The actual stress in the gage section (numerator of Eq. 3.2) during the elastic phase of the loading (approximately 50 ksi) was determined by multiplying the strain from the strain gage by the modulus of the material obtained from the uni-axial tests.

The applied load was divided by the cross-sectional area at the grips to determine the applied stress (denominator of Eq. 3.2).

The BCF was calculated for each geometry and direction of loading (X and Y) based on an average of 3 tests for each case.

Once the BCF was determined the actual stress in the gage section was determined by multiplying the applied stress with the BCF.

$$BCF = \frac{stress\ in\ gage\ section}{applied\ stress} = \frac{(Modulus)_{effectiv}\varepsilon_{measured}}{(Load)_{measured}/(Area)_{Measured}} \quad \text{Eq. 3.2}$$

3.8 SUMMARY

This section outlined the design of the control and shimmed specimens. It also described the specimen fabrication process and material characterization of the materials. The material characterization included the following tests: Ultimate tensile strength, density, void ratio, and fiber volume content. The bi-axial test procedure was also described. The results from these tests are described in Section 4.

Section 4

EXPERIMENTAL RESULTS

4.1 DENSITY AND FIBER VOLUME CONTENT

The fiber volume and related quantities are shown in Table 4.1. The importance of determining these properties is to better understand the material being used. It also gives the researcher information that can be used in future calculations.

4.2 UNI-AXIAL TENSION TEST

Averaged result data for both lay-up configurations can be seen in Table 4.1 for the IM7/UF3352 material. Handbook values were used for the properties of the IM7/PATZ material. Shown in the table are the values determined experimentally as well as the values determined from Composite Laminate Theory (CLT).

Table 4.1: Results from uni-axial tension test w/ CLT results.

Lay-up Config:	$[(0/90)_8]_s$ exp.	$[(0/90)_8]_s$ CLT	$[(0/90)_4(45/-45)_4]_s$ exp.	$[(0/90)_4(45/-45)_4]_s$ CLT
E_t (ksi)	11800	11000	7200	7473
Fu_t (ksi)	120	N/A	87	N/A
ν	0.015	0.01	0.31	0.26

The first two specimens, $[(0/90)_8]_s$ failed in the wedge grips, having LAB (Lateral At grip/tab Bottom) failure. This undesired failure occurred due to the larger thickness than specified in the standard. A stress strain diagram of one of the first two tests can be seen in Figure 4.1.

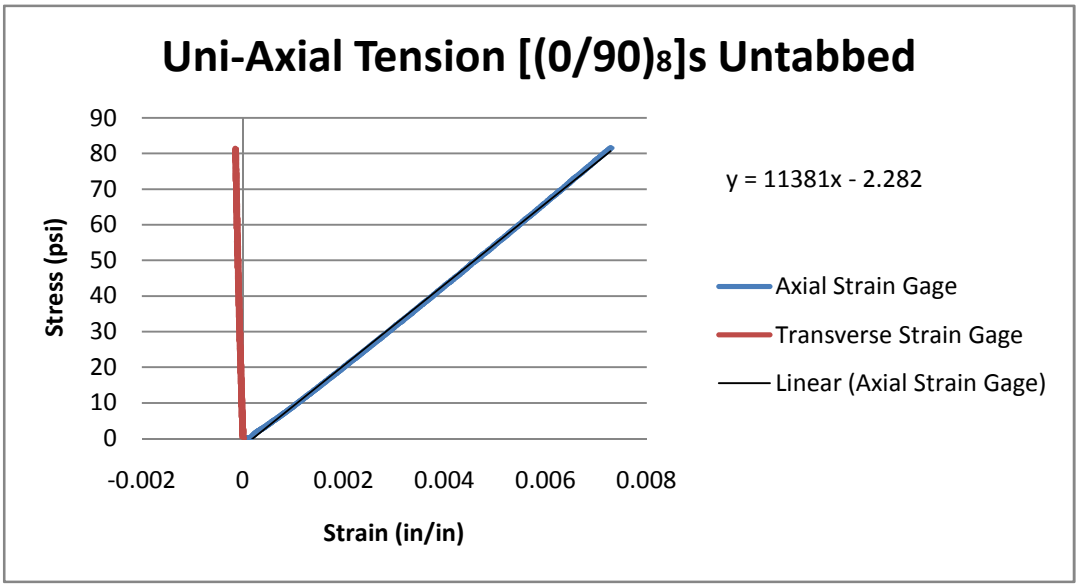

Figure 4.1: Uni-Axial test data for one of the wedge grip failures.

As shown in Figure 4.1 the failure occurred at about 80ksi with a modulus of about 11,000ksi. The Poisson's ratio was 0.014, which compared favorably with the composite laminate theory calculated value of 0.01.

This low Poisson's ratio was due to the percentage of fibers in the longitudinal direction. Since this particular lay-up had half of the fibers in the longitudinal direction and half in the axial direction it causes a small Poisson's ratio. As the percentage of +-45˚ plies goes down with so does the Poisson's ratio. The carpet plot shown below contains a drawn in line for the $[(0/90)_4(45/-45)_4]_s$ lay-up configuration and the resulting Poisson's ratio of 0.3. The other lay-up configuration, $[(0/90)_8]_s$ has 0% 45˚ plies and 50% 0˚ plies which results in a Poisson's ratio close to 0.03. This can be seeing in the carpet plot shown in Figure 4.2.

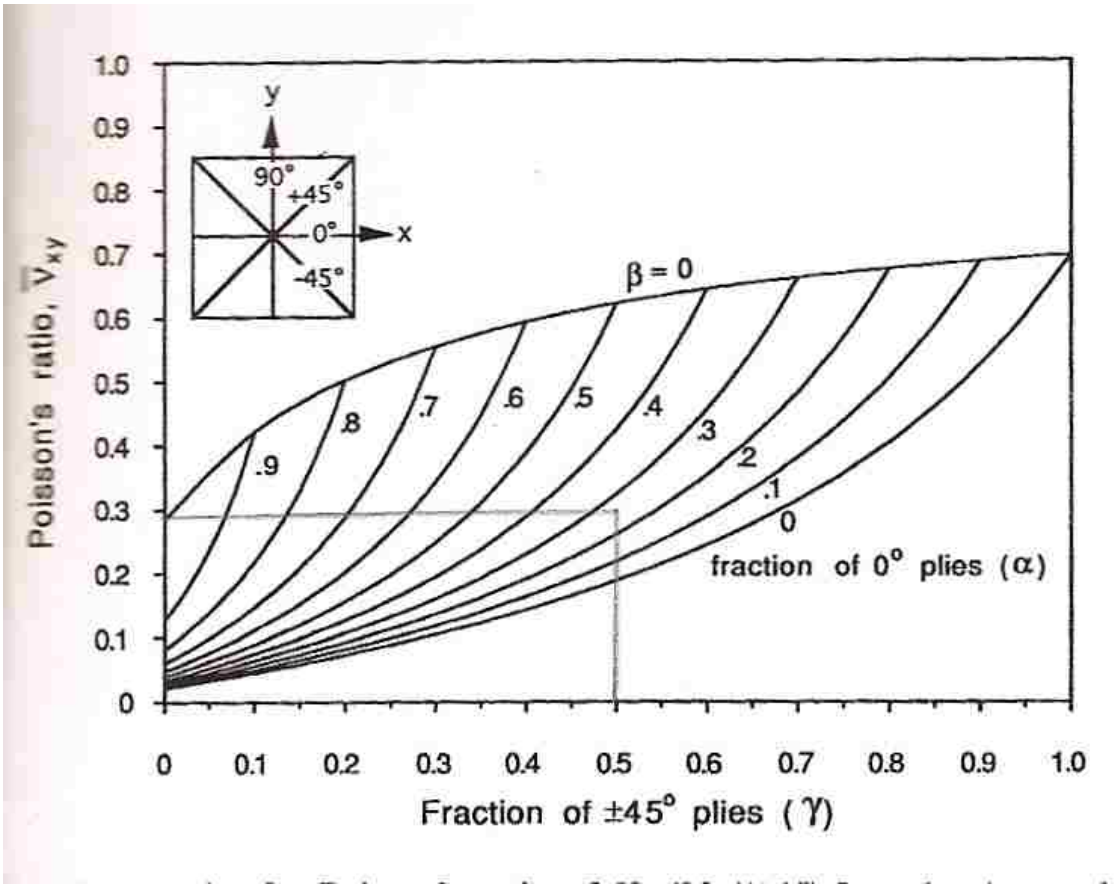

Figure 4.2: Shows a carpet plot of fraction of 0˚, and +-45˚ plies and the corresponding Poisson's ratio [14].

G10 glass-epoxy tabs were bonded to the specimens to help prevent further wedge grip failures. The tabs were attached with Hysol 9309 epoxy adhesive. The tabs were clamped with spring clamps during curing. A picture of this process is shown in Figure 4.3.

Figure 4.3: Uni-axial specimens with G10 glass tabs clamped for adhering.

The specimens with the glass tabs were then cured in oven at a temperature of 185˚F for a period of 6 hrs. The remaining specimens were then tested. Figure 4.4 and Figure 4.5 show the data obtained for one of the 90 lay-ups and one of the 45 lay-ups, with tabs, respectively.

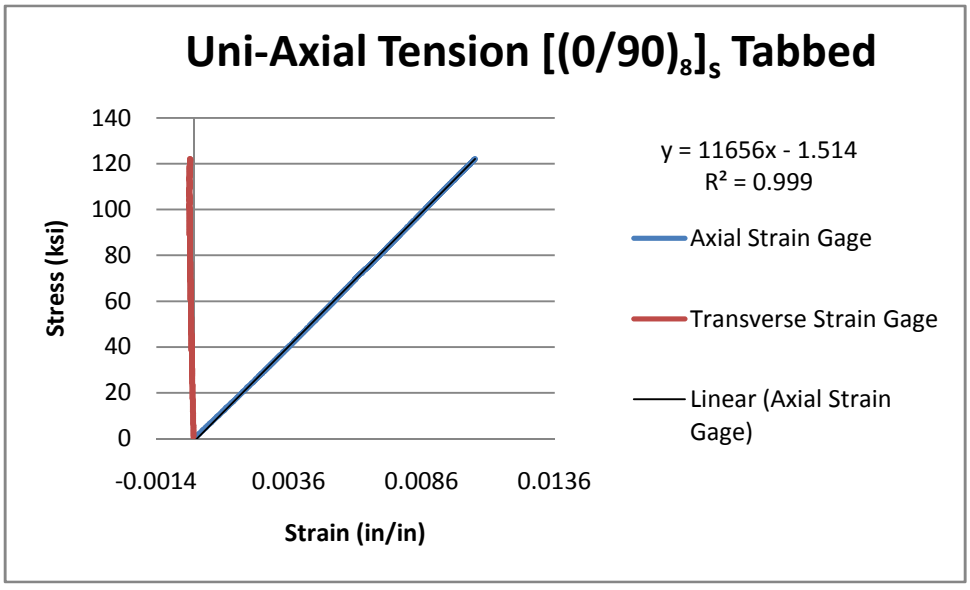

Figure 4.4: Uni-Axial tension data for tabbed $[(0/90)_8]s$.

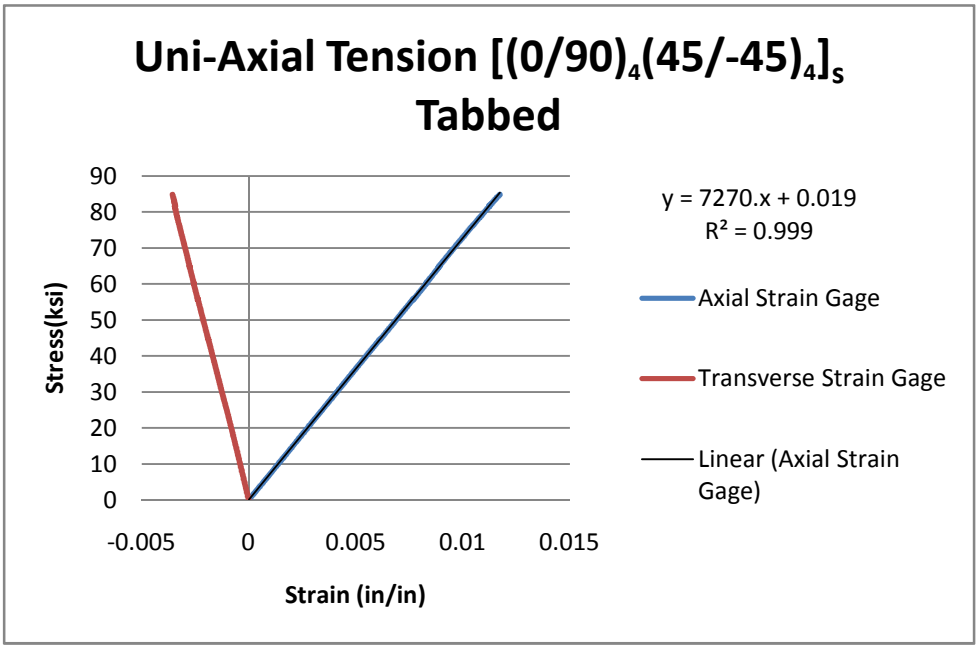

Figure 4.5: Uni-Axial tension data for tabbed $[(0/90)_4(45/-45)_4]s$.

As shown in Figure 4.4 the $[(0/90)_8]_s$ laminate failed at about 120 ksi with a modulus of 11,600 ksi. The $[(0/90)_4(45/-45)_4]_s$ laminate, which was not initially tested, had a failure strength of 85 ksi. This is due to fewer fibers in the axial direction of loading. However, both of the tabbed specimens still exhibited LIB (Lateral Inside grip/tab Bottom), LAB (Lateral At grip/tab Bottom), and MAB (Multi-mode At grip/tab Bottom) failures. The MAB failure type can be seen in Figure 4.7. The mixed mode is a combination of two angled failures and a bit of explosive failure that is at the wedge grip. Untabbed LAB failure can be seen in Figure 4.6.

Figure 4.6: Untabbed uni-axial LAB failure in wedge grip.

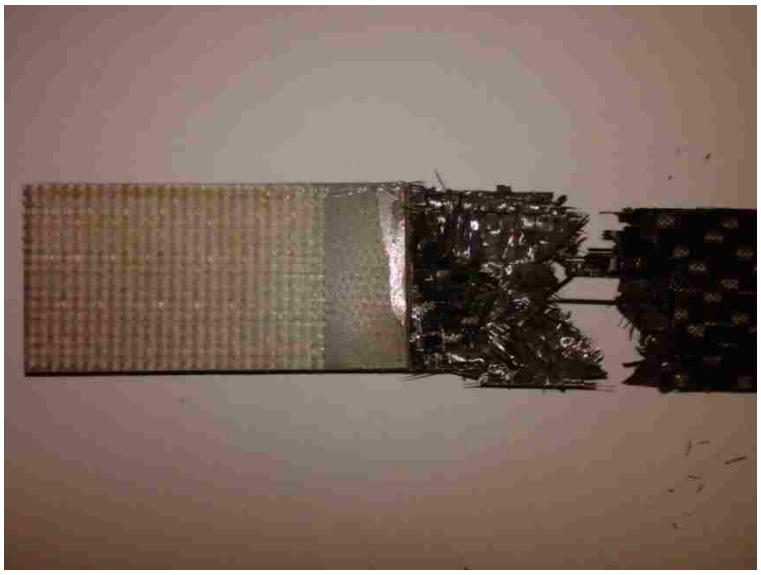

Figure 4.7: Tabbed uni-axial MAB failure.

These types of failures are undesirable because the specimens are not failing in the middle, and are still close to the wedge grip. This leads the author to believe that the specimen thickness is too large for this test and cannot be corrected by the use of tabs. These failures help validate the geometry recommendations found in the ASTM standard.

All of the test specimens yielded this type of failure. The data can be found in Appendix A.

4.3 BI-AXIAL TESTING

Bi-axial testing for this research was done in accordance to the bi-axial procedure described previously in Section 3.6. A set of three different specimens for each the shimmed specimens and the control specimens were tested with a 1/1 load ratio along the X and Y axes. Typical gage-section stress-strain data are shown in Figures 4.10 and 4.13. The gage section stress values were obtained using the Bypass Correction Factors (BCF) described earlier. The results of all of the Type I tests can be seen in Table 4.4.

Table 4.2: Failure data for Type I tests.

Type I Tests		
Specimen Name	Ultimate Stress X (ksi)	Ultimate Stress Y (ksi)
Control-1	113.6	107.6
Control-2	108.9	108.5
Control-3	114.97	113.6
Average	**112.49**	**109.9**
BCF	*1.14*	*1.14*
CV (%)$_{control}$	2.83%	2.94%
Shimmed-1S	81.7	55.7
Shimmed-2S	83.3	51.7
Shimmed-3S	82.4	49.9
Average	**82.47**	**52.43**
BCF	*0.91*	*0.87*
CV (%)$_{shimmed}$	0.97%	5.66%

A picture of a failure can be seen in Figure 4.8.

Figure 4.8: Failure of a Type I control bi-axial specimen.

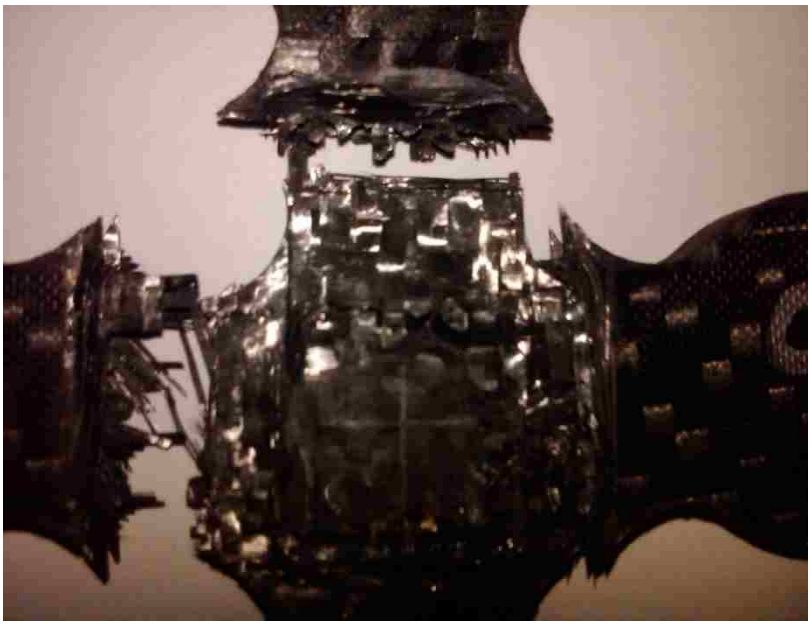

Figure 4.9: Close up of failure in the Type I control specimen.

As shown in Figure 4.8 and 4.9, failure is not in the gage section. The failure is occurring outside the biaxial loaded region. A stress-strain diagram with both direction loadings is shown in Figure 4.10, which shows how the material reacts in a stressed state.

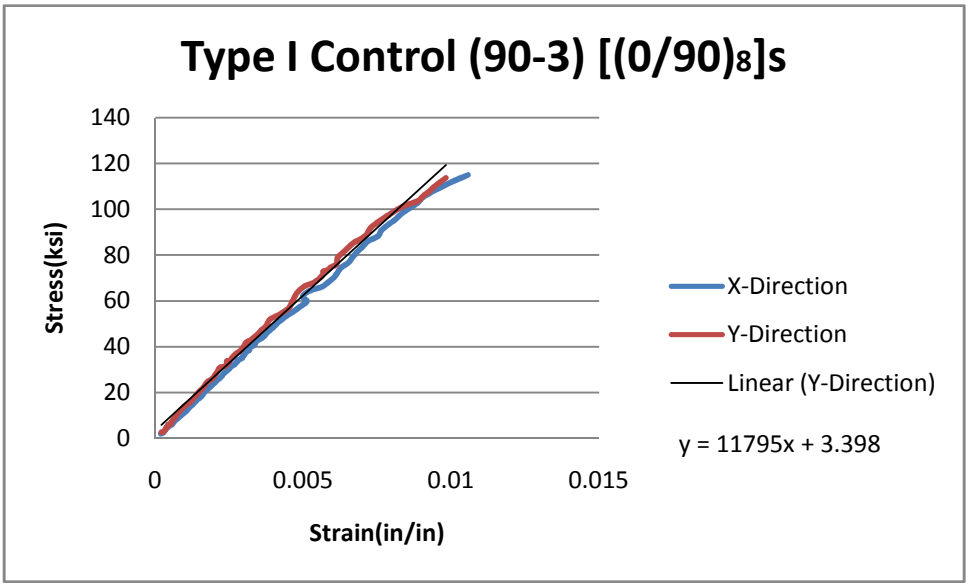

Figure 4.10: Stress strain diagram of a bi-axial control specimen.

As shown in the above stress-strain diagram the specimen failed at about 115 ksi. This failure strength is less than that of the uni-axial specimen of the same lay-up configuration, $[(0/90)_8]_s$. Three shimmed specimens were also tested under the same load ratio and a picture of the failure can be seen in Figure 4.11.

Figure 4.11: Shows a Type I shimmed bi-axial specimen failure.

Figure 4.12: Close up photo of the Type I shimmed failure.

The failure of the shimmed specimens occurred at the same location as the Type I control specimens. Failure is not in the gage section but is also not at the narrowest section of the arms (Figures 4.11 and 4.12). A typical stress strain diagram for one of the shimmed specimens is shown in the below figure. 90-3s is shown below because it was the best data obtained for the Type 1 shimmed specimen. All of the data can be seen in Appendix C.

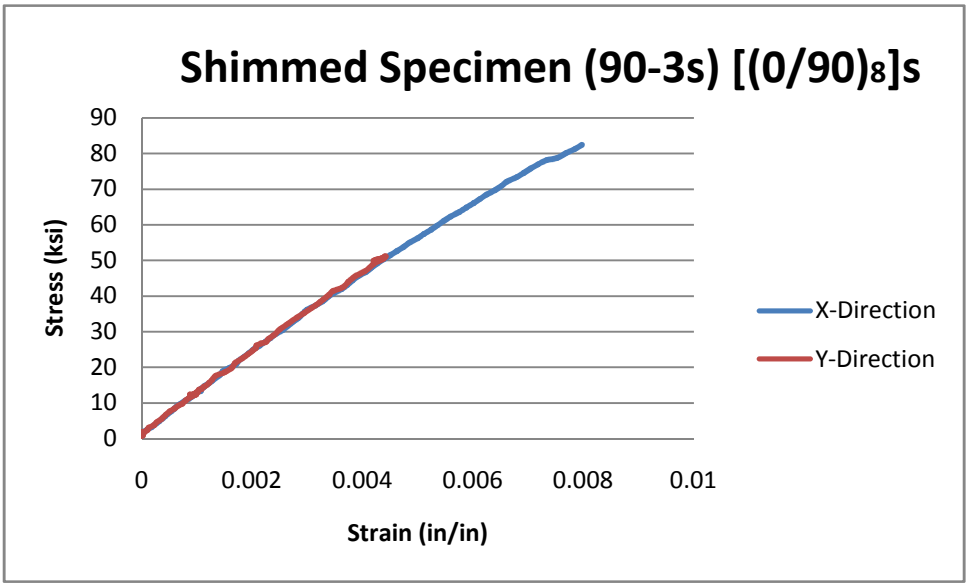

Figure 4.13: Stress strain diagram of a bi-axial shimmed specimen.

The ultimate failure strength of this particular shimmed specimen, 90 ksi, was about 10 ksi less than that of the control specimens. Also, notice that the data stopped at 50 ksi for the Y-Direction. This sort of behavior was seen across all three of the shimmed specimen failures. This is happening because of damage initiation due to the abrupt change in thickness from the addition of the shim. When compared, the shimmed specimens are failing at a slightly lower stress than the control specimens. Failure data

for both of the control and the shimmed specimens, Type I test, can be seen in Figure 4.14.

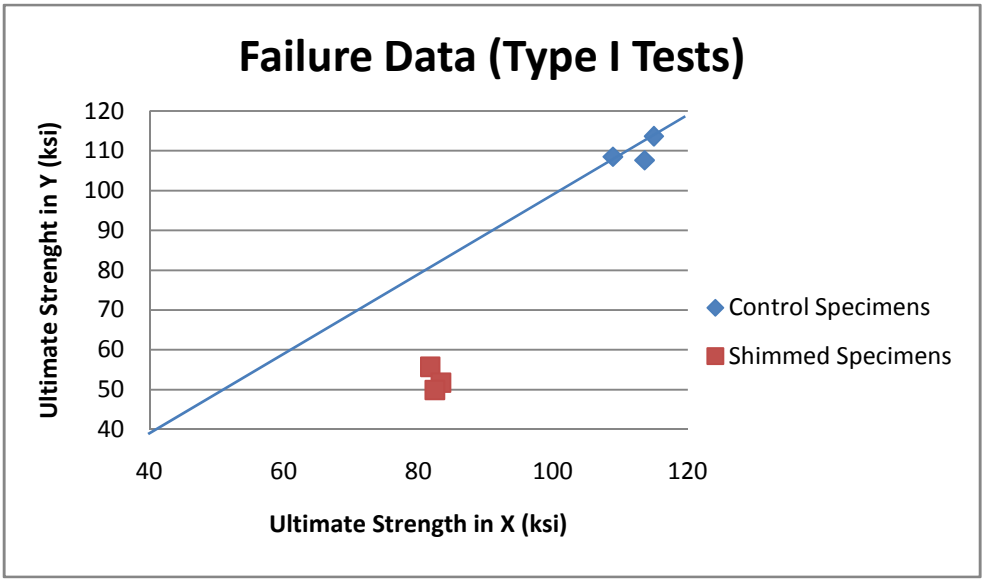

Figure 4.14: Failure data for both control and shimmed specimens.

Plotting both the shimmed and control specimens together shows the separation between the two design configurations. Both of the two designs have a close grouping with one another, with a coefficient of variation of 22% for the X-direction and 50% for the Y-Direction. Also shown on the graph is a line representing a 45˚ angle. This shows how the specimens are failing relative to each direction. If the specimens fail on this line, it would mean that the specimens are failing at the exact same load in both directions and no damage is occurring in either direction before the other. Since the ultimate failures for the Y-direction are not near the line they are failing in one direction and still being able to take load in the opposing direction. This shows that one axis contains damage before the other. This can be seen better in Figure 4.15.

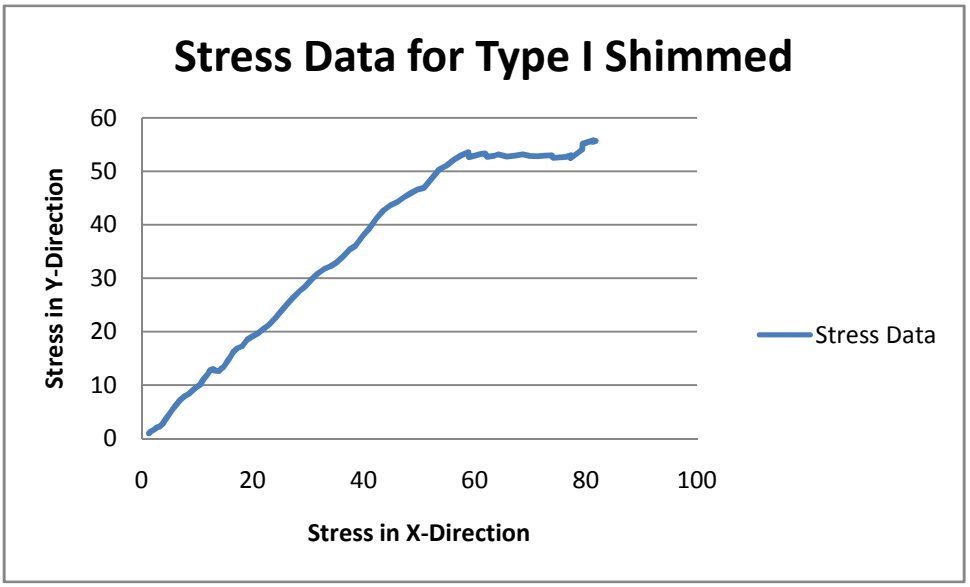

Figure 4.15: The stress in both the X and Y directions for Type I Shimmed.

The plot shown in Figure 4.15 is consistent with all Type I shimmed specimens. Therefore, damage in the Y-direction is causing the specimen to fail at less stress in that direction.

4.4 DISCUSSION

Overall, the shimmed specimens failed undesirably. The shimmed specimens failed at the stress concentration caused by the shims (Figure 4.15). The failure always occurred just below the narrowest section in the Y-direction. However the Type I control specimens did not fail in the gage section either, but are still providing lower limit test data. Overall, the Type I specimen geometry was not an adequate cruciform geometry since it had undesired failure for both the shimmed and the control specimens. Damage can be occurring first in the Y-direction for the shimmed specimens due to alignment issues in the wedge grips. Due to the thickness of the specimens the wedge grips had to be moved back, only for the Y-direction, in order to fit the specimen into the machine.

This could have caused misalignment in the Y-direction, which could cause damage to occur first in that direction.

Overall, the specimens were uncharacteristically thick and made out of woven carbon fiber-epoxy material which didn't seem to have any affect in the results of this research. The change in geometric shape design of the specimens should have been kept to what is already used for bi-axial research at the AFRL [6].

4.5 TYPE II TESTS SPECIMEN FABRICATION

Due to the original specimens' undesired failure modes, an additional design was added to this research. The first change to the specimens was a fall back to the AFRL's original geometric design. The specimens were still made out of a woven carbon fiber-epoxy composite, but instead of aluminum shims, a built-up panel design was used. The intent of the built-up design was to avoid the abrupt change in area where the shims meet the composite. It was deemed better to cover the entire specimen with this additional material to prevent the stress concentration seen in the Type I shimmed specimens. Before the composite plate was machine it was sandwiched between two G10 glass fiber panels. The changes made in this research from what was previously done by Ash and Welsh [1], are as follows: The thickness of the G10 material previously used was 0.062 in. and the new thickness is 0.093 in. This was done to gain a similar thickness as in the Type I tests. The adhesive previously used was Hysol 9309 and the new adhesive is a Hysol .03 in. film adhesive (Henkel Corperation, Bay Point, California) that was post cured to the composite plate. The previous Hysol 9309 is a two part epoxy adhesive that is spread on to the plate by hand. This hand spreading is not an efficient way of adhering

large panels together, as it can allow large amounts of trapped air into the bonding surface. The Hysol .03 in. film adhesive is cut to the size of the plate and placed in between the composite and the G10 then cured simultaneously with the composite laminate. The use of the film adhesive reduces the amount of trapped air or space that is lacking adhesive epoxy. Control specimens were also machine out of the same woven composite material used in the center of the built-up panel. A picture of the two new specimens can be seen below.

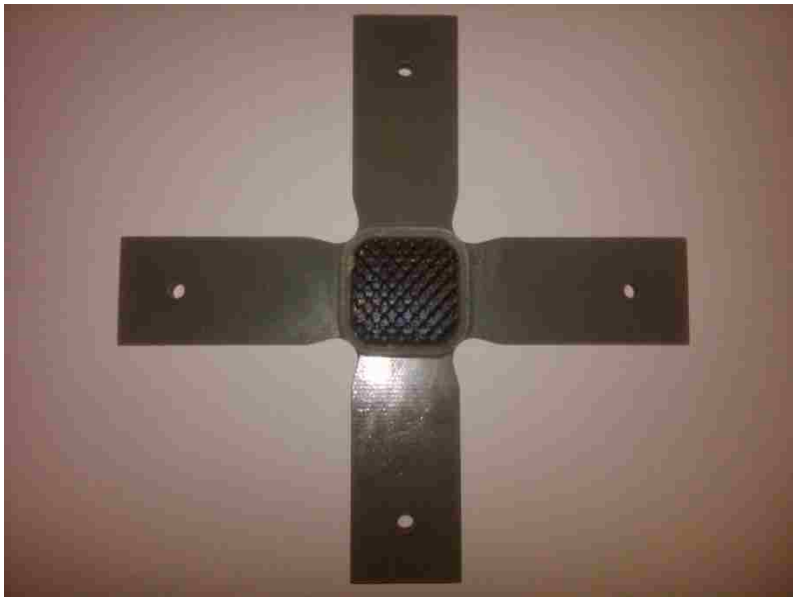

Figure 4.16: New Type II built-up panel specimen.

Figure 4.17: Type II standard tapered thickness cruciform specimen.

The material used in this case is a plain weave IM7/PATZ. The PATZ epoxy is the manufactures equivalent to a 977-2 epoxy. The lay-up configuration for the laminate in the built-up specimens is $[(0/90)_2]s$ and the Type II control is $[(0/90)_3]s$. Overall, this newly added design should show equivalent or better results than the previous design.

4.6 RESULTS ON TYPE II TESTS

Overall, the new built-up panel configuration greatly improved the failure of the specimens. All specimens, including the control, exhibited failure in the gage section. All failures initiated in the gage section, where the specimen is experiencing bi-axial loads. Ultimate failure strengths can be seen in the below table.

Table 4.3: Ultimate failure stress for the Type II tests.

Type II Tests		
Specimen Name	Ultimate Stress X (ksi)	Ultimate Stress Y (ksi)
Control-1	111.3	104.1
Control-2	105.9	93
Control-3	102.3	105.8
Average	**106.5**	**100.97**
BCF	*1.67*	*1.72*
CV (%)$_{control}$	4.25%	6.88%
Built -Up-1	94.1	93.4
Built -Up-2	78.8	79.1
Built -Up-3	85.5	84.6
Average	**86.13**	**85.7**
BCF	*2.06*	*2.06*
CV (%)$_{Built-Up}$	8.97%	8.42%

From the desired failure mode it can be concluded that these specimens were adequately designed. A picture of both the control failures and the built-up failures are shown in the respective figures below.

Figure 4.18: Adequate 45˚ failure mode for the Type II control specimen.

Figure 4.19: Adequate 45˚ failure mode for the Type II built-up specimen.

Shown in both figures above is a 45˚ failure line exhibited from the top right corner to the bottom left corner. This is an ideal failure mode for a bi-axial cruciform

specimen for a 1/1 stress ratio. The left arm failure (Figure 4.18) in the control specimen was a post fracture failure due to the crack in the gage section. The arm fractures off once the initial crack propagates to the bottom left corner of the arm, weakens that arm which fractures shortly after the main failure. Stress-strain diagrams for both the control and the built-up specimens can be seen below respectively. A failure data graph is also shown in Figure 4.22.

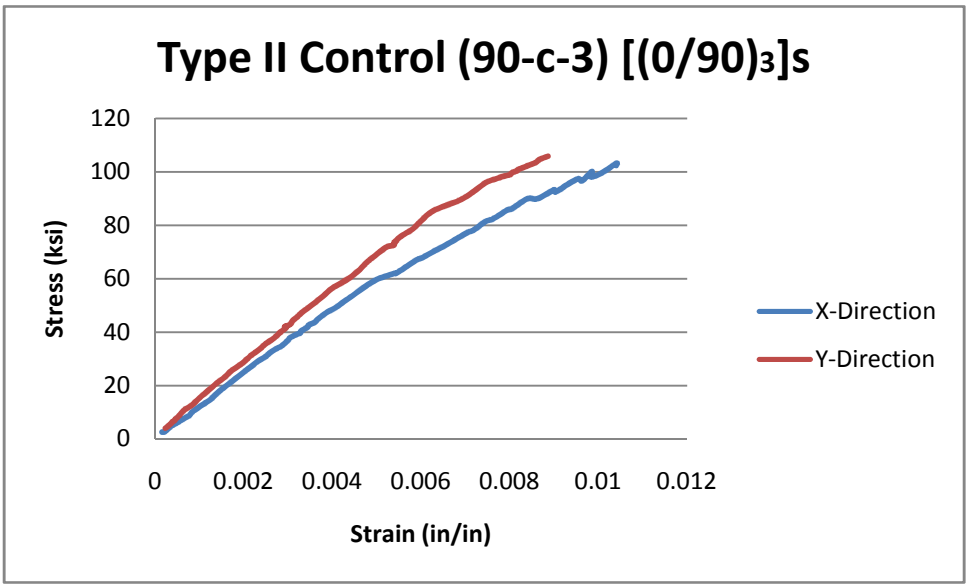

Figure 4.20: Type II control specimen stress-strain diagram.

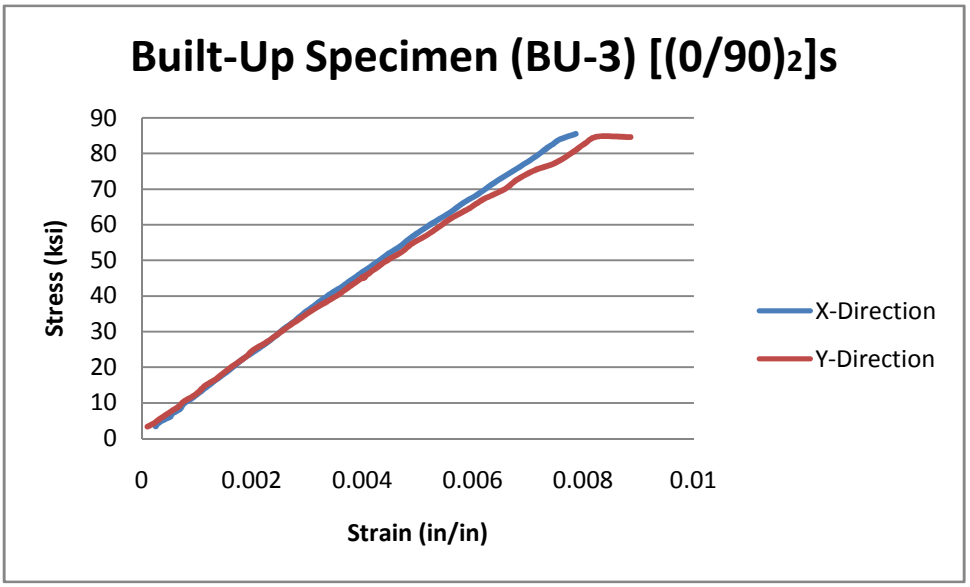

Figure 4.21: Type II built-up panel specimen stress-strain diagram.

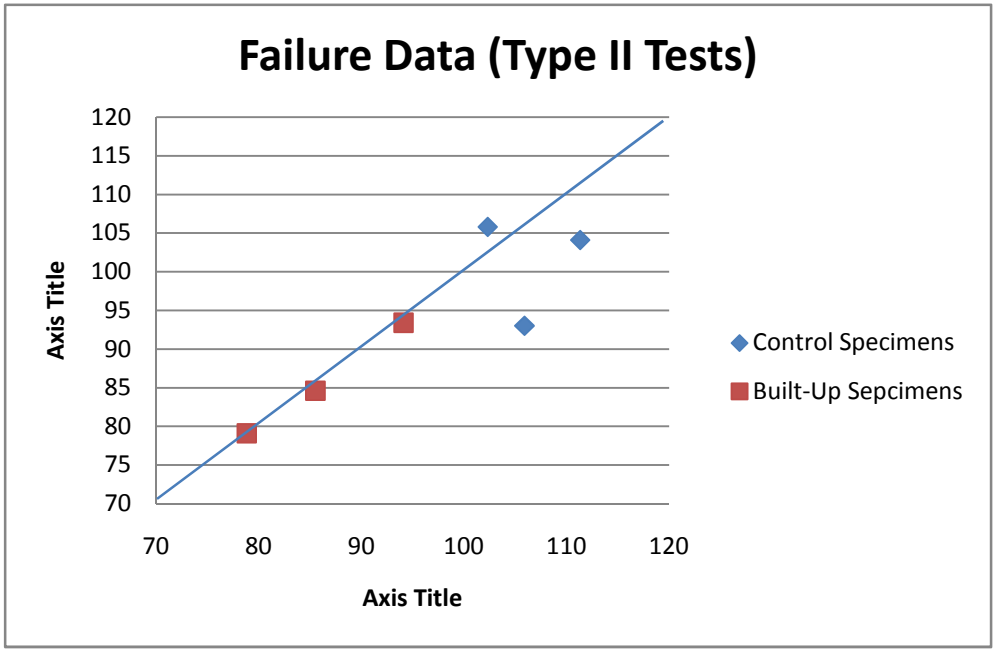

Figure 4.22: Failure data for Type II test specimens.

The failure data shown is shows a good representation of the Type II specimens and how they are similar. The stress in the X and Y directions at failure are close, with a

15% coefficient of variation in the X-direction and 11% in the Y-direction. The reason for the slight difference between the Type II control specimens and the Type II built-up specimens is primarily due to the thickness of the gage sections. The thickness in the built-up gage section is slightly thicker, 0.064 in, than that of the Type II control specimen, 0.048 in. The thinner the gage section the higher the overall stress. Also, shown in Figure 4.22 is the 45˚ line representing the 1/1 load ratio failures. In this graph, all of the built-up failures are on that line. This shows that failure is occurring in the gage section where the specimen is loaded in both directions simultaneously, and there is no preferential damage in either direction prior to failure. Type II control specimens however are not failing at the same loads in both directions. Type II control specimens have a coefficient of variation of 33% between the X-direction failure and the Y-direction failure, while the built-up specimens only have a 4% coefficient of variation. A plot representing the two stress directions for the Type II control specimens can be seen below.

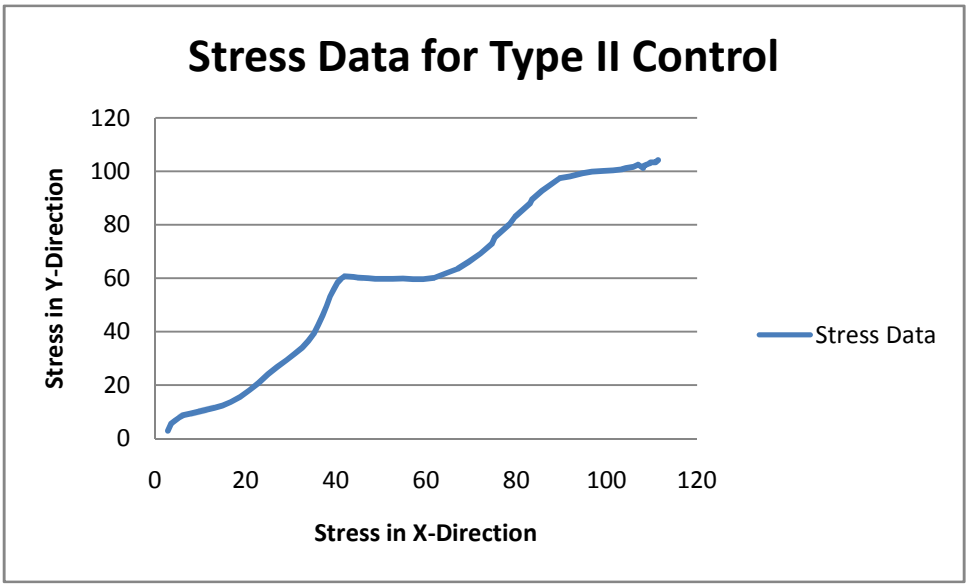

Figure 4.23: The stress in both the X and Y directions for Type II control Specimens

Shown in Figure 4.23 is similar results as in the previous Type I shimmed specimens. Damage is occurring in the Y-direction for two of the specimens and the X-direction for the remaining specimen, which is causing premature failure in that direction. Since the Type II control specimens are not as thick as the Type I specimens the wedge grips were not required to be moved back to fit into the testing machine. The damage occurring initially for the Type II control specimens is happening due to another reason. This could be due to minor misalignment issues in the actuators rather than the wedge grips.

4.7 CENTER HOLE SPECIMENS

A study was conducted on the effect of a center hole stress concentration in the Type I specimens. A ¼" hole was drilled directly in the center of three Type I control specimens and three Type I shimmed specimens. These were then tested in the same bi-axial test facility, as before, under a 1/1 load ratio. A three dimensional FEM was done

on the two geometries with the center hole prior to testing. The resulting FEM analysis can be seen below.

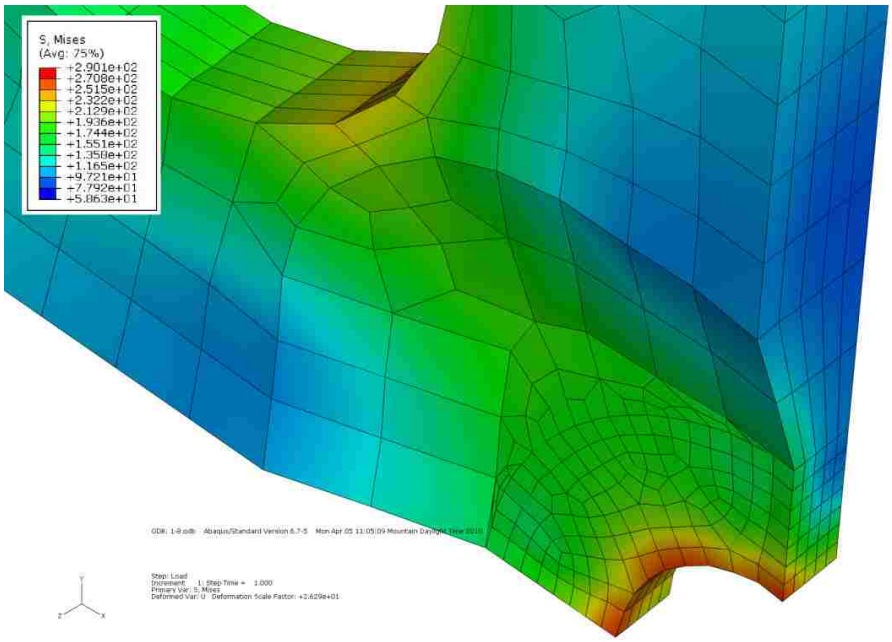

Figure 4.24: FEM of the Type III control specimen with a ¼" center hole.

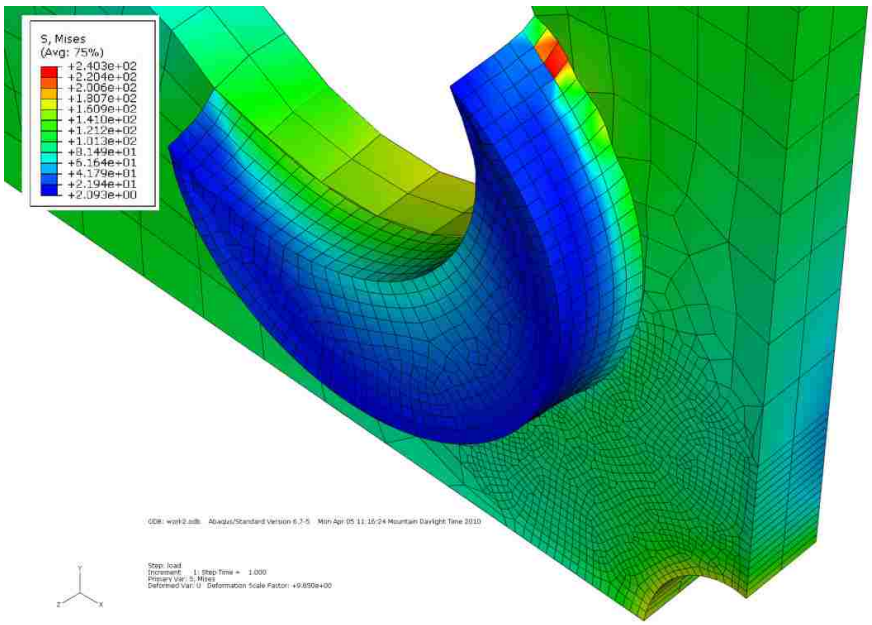

Figure 4.25: FEM of the Type II shimmed specimen with a ¼" center hole.

The FEM for the Type III control geometry shows a stress concentration factor around the hole of 3. The stress concentration around the hole in the Type III shimmed specimen is 2. The difference in stress concentrations is possibly due to the change in the stress field due to the addition of the shims. The FEM of the Type III control shows the stress plot following a 45˚ angle from the X and Y directions (Figures 4.24). The Type III shimmed specimen FEM didn't show this 45˚ stress plot due to the stress concentration occurring at the cusp of the shim. The below Figures below show how the specimens failed under a 1/1 bi-axial loading condition.

Figure 4.26: Center hole Type III control specimen failure.

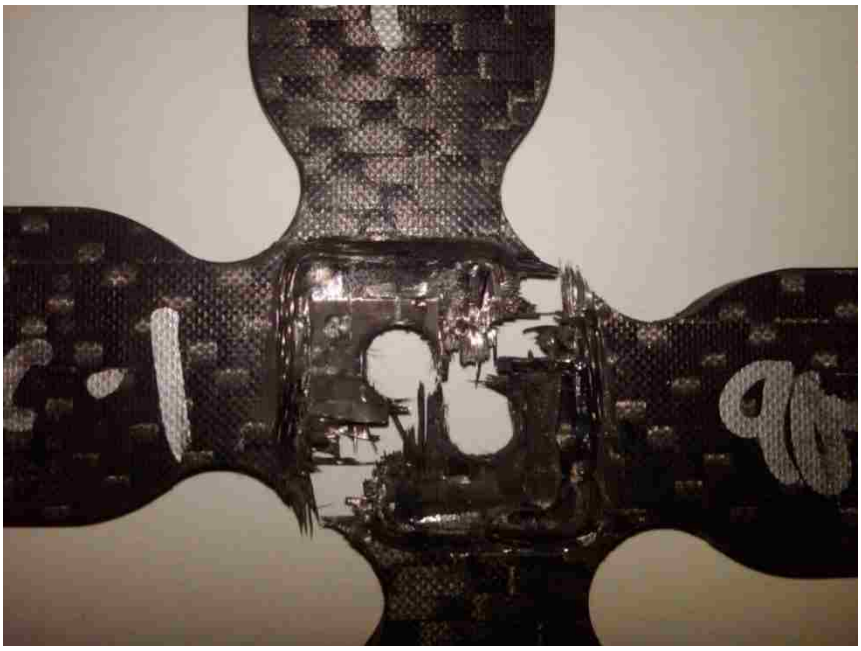

Figure 4.27: Center hole Type III control specimen complete separation failure.

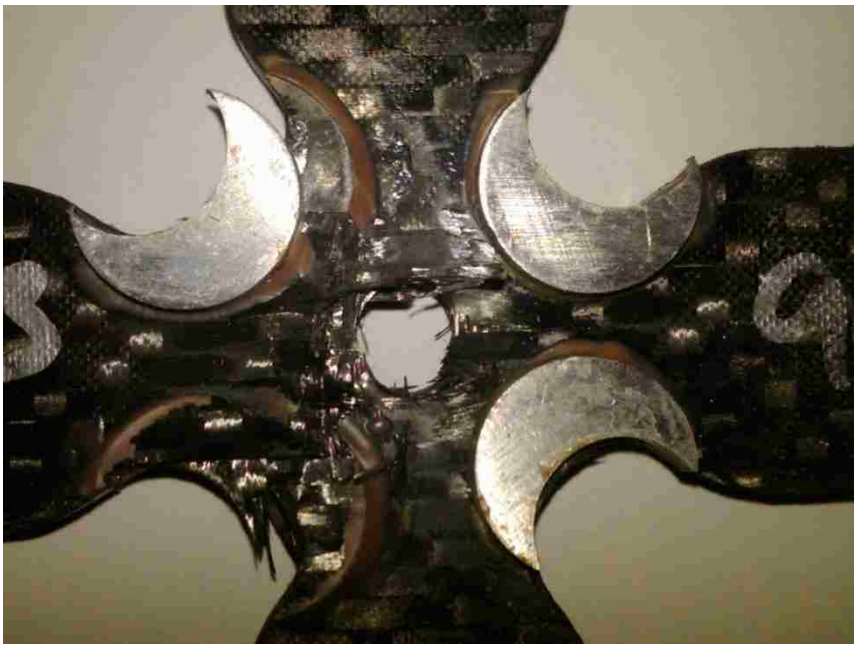

Figure 4.28: Center hole Type III shimmed specimen failure.

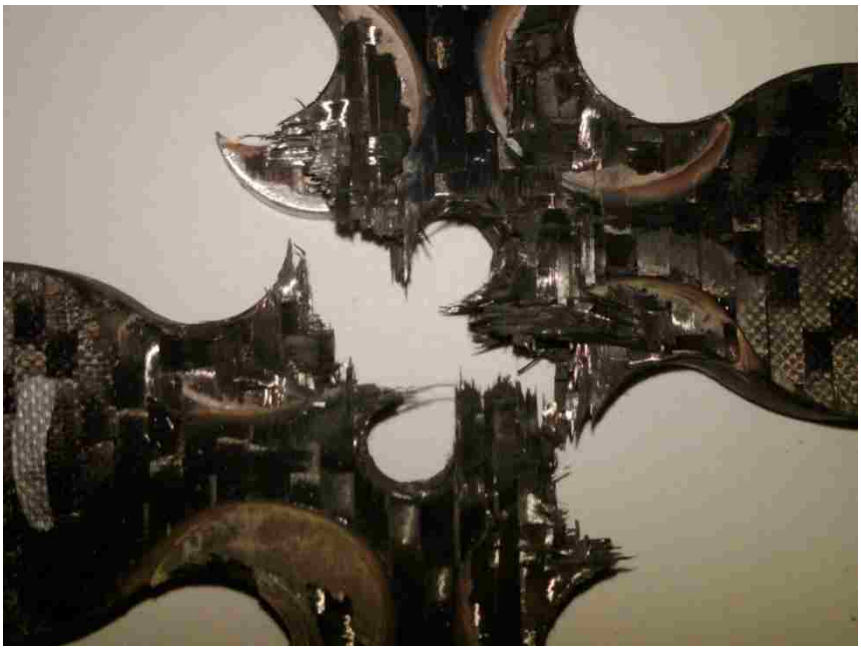

Figure 4.29: Center hole Type III shimmed specimen complete separation failure.

All specimens exhibited failure along a 45˚ fracture line as predicted by the FEM analysis. A table showing the failure stress and how they compare to that of a non-hole specimen is shown below.

Table 4.4: Ultimate failure strss of Type III tests.

Type III Tests				
Specimen Name	Ultimate Stress X w/ hole (ksi)	Ultimate Stress Y w/ hole(ksi)	Strength Reduction Ratio in X (%)	Strength Reduction Ratio in Y (%)
90-1-h	79.9	80.6	29.67%	25.09%
90-2-h	79.7	73.1	26.81%	32.63%
90-3-h	78.3	75.8	31.90%	33.27%
Average	**79.3**	**76.5**	**29.46%**	**30.33%**
CV (%)$_{control\text{-}hole}$	1.10%	4.97%	8.65%	15.00%
90-1S-h	58.8	57.5	28.03%	-3.23%
90-2S-h	67.6	57.3	18.85%	-10.83%
90-3S-h	62.7	52.9	23.91%	-6.01%
Average	**63.03**	**55.9**	**23.59%**	**-6.69%**
CV (%)$_{shimmed\text{-}hole}$	7.00%	4.65%	19.49%	-57.46%

From the results shown in the above table the overall strength of the specimens are reduced by 30% for the Type III control specimens and 24% for the Type III shimmed specimen. The shimmed specimens, which already had a strength reduction due to the shims did not show further strength reduction due to the hole. Recall from Type I shimmed tests data that the shimmed specimens failed in the Y-direction at an average of 52 ksi due to the addition of the shim. Theoretical values for the stress concentration around a hole an infinite element under biaxial tensile loading has a stress concentration value of 2 [15]. A stress concentration of 2 would cause a strength reduction ratio to be 50%. In the Type III control specimens there is a strength reduction of 30% which corresponds to a stress concentration of 1.4. The test data is actually closer to that of the theoretical stress concentration of 2 rather than the stress concentration value of 3 obtained from the FEM. The difference between the actual data, FEM and the theoretical could be that the theoretical analysis is based on an infinite plate with a hole.

Section 5

CONCLUSIONS AND RECOMMENDATIONS

5.1 CONCLUSIONS

The results from this research have led to several conclusions about developing a modified bi-axial composite test specimen. Along with additional conclusions on the effect of a stress concentration around a hole drilled in the center of the same cruciform geometry. The following conclusions are summarized below:

- Aluminum shims caused damage to occur at the edge of the shims due to high stress concentrations.
- New biaxial failure data was obtained for thicker specimens that is currently available.
- Biaxial failure data not currently available was obtained for woven carbon fiber-epoxy cruciform specimens.
- Even though the Type I specimens failed outside the gage section, the data provides a reliable lower limit for thick woven carbon fiber-epoxy cruciform specimens.
- Type II built-up panel configuration yielded ideal failure modes.
- Type II control specimens had damage initiating in Y-Direction which caused lower failure strengths in the same direction.
- Type III tests with center holes drilled in the gage section exhibited a strength reduction of the specimens by 30%.

- Type III shimmed specimens had no strength reduction due to the previous strength reduction from the stress concentration around the shim

The main objective of this research was to limit the amount of machining done on the typical cruciform bi-axial test specimen. Type I control geometry yielded good results but failure did not occur in the gage section. The shimmed specimens failed at a much lower stress due to the stress concentration from the added shims. Due to these undesired failures only the $[(0/90)_8]s$ lay-up configuration was tested. Due to the inaccurate failures in the Type I tests, a built-up panel configuration was fabricated and tested [1]. The outcome of the Type II built-up specimens were completely ideal failures. The Type II control specimens however had damage in the Y-Direction which caused lower failure strengths in the same direction. Type II specimens were also fabricated out of a woven carbon fiber-epoxy material as well as being thick specimens. A ¼" hole was drilled in Type I shimmed and control geometry to determine what the effect of a hole stress concentration in a cruciform specimen would be. The addition of the center hole test, Type III tests, produced a strength reduction of 30%. The stress concentration from theoretical results suggests a value of 2, while FEM suggest a stress concentration value of 3. The actual stress concentration obtained from Type III tests was a value of 1.4. This is close to that of the theoretical value but differs due to the theoretical value being that of a hole in an infinite plate under bi-axial loading.

An important lesson learned from this research is that designs based on analyses/FEM don't always turn out as planned in the lab. The initial shimmed and control specimens didn't fail as desired. Since AFRL was in the process of machining composites, the author was able to fabricate more plates to add the built-up panel

configurations to the research. Also, due to the initial geometries not working too well, the author used additional specimens to add the Type II tests. The hands on experience of fabricated and testing the specimens was an invaluable experience learned during this research.

5.2 RECOMMENDATIONS

For further research into the development of a modified bi-axial composite test specimens the author recommends the following:

- Use previous geometries that are known to exhibit ideal bi-axial failure.
- If using shims, as described in this research, taper the thickness to remove stress concentrations at the bond edge.
- Use a built-up panel configuration with a film adhesive. The use of a film adhesive showed better results than the use of an epoxy.
- For the center hole specimens, the author recommends different hole diameters to see how a change in hole diameter also changes the strength reduction ratio.

APPENDICES

APPENDIX A: IM7/UF3352 MATERIAL PROPERTIES

APPENDIX B: IM7/PATZ AND G10 MATERIAL PROPERTIES

APPENDIX C: BI-AXIAL TEST DATA

APPENDIX A: IM7/UF3352 MATERIAL PROPERTIES

- Density=1.49g/cm^3
- Fiber Volume=49.2%
- Void Volume=.2%

Density/Fiber Volume/Void Content data shown below:

Water Temp (deg C):	16.5
Water Density (g/cc):	0.9988634
Resin Density (g/cc):	1.208
Fiber Density (g/cc):	1.795

	Dry Comp.	Wet Comp.	Fiber	Resin	Composite	Fiber	Resin	Void	Resin
Specimen	Weight (g)	Weight (g)	Weight (g)	Weight (g)	Density (g/cc)	Volume (%)	Volume (%)	Volume (%)	Conten (%)
1	0.9160	0.3021	0.5407	0.3753	1.4904	49.0	51.0	0.4	41.0

2	0.9149	0.3076	0.5454	0.3695	1.5048	50.0	50.0	-0.3	40.4
3	0.9196	0.3021	0.5404	0.3792	1.4875	48.7	51.3	0.5	41.2
				Average	**1.49**	**49.2**	**50.8**	**0.2**	40.9
				Stdev.	0.01	0.67	0.67	0.44	0.43
				CV (%)	0.62	1.35	1.31	196.68	1.06

Six uni-axial tension tests were done, three on each lay-up configuration. Two tests on the $[(0/90)_8]s$ lay-up showed wedge grip failure. G10 tabs were adhered as discussed earlier in the research and also demonstrated wedge grip failure. All of the stress-strain diagrams are shown below. The 90 and 45 designation signifies the lay-up configuration; 90 designating the $[(0/90)_8]s$, and 45 designating the $[(0/90)_4(45/-45)_4]s$. The number that follows the 90 or 45 represents the test number.

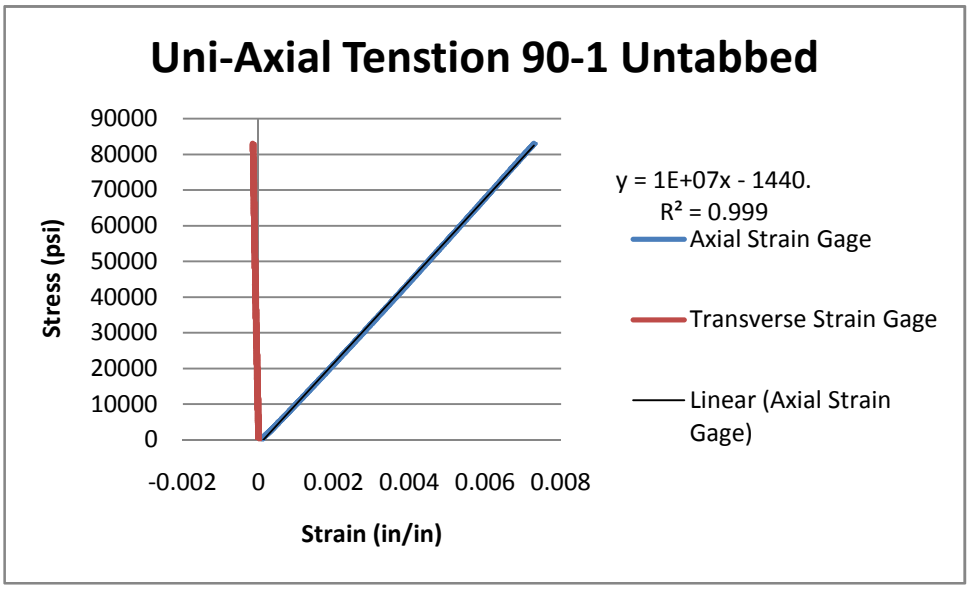

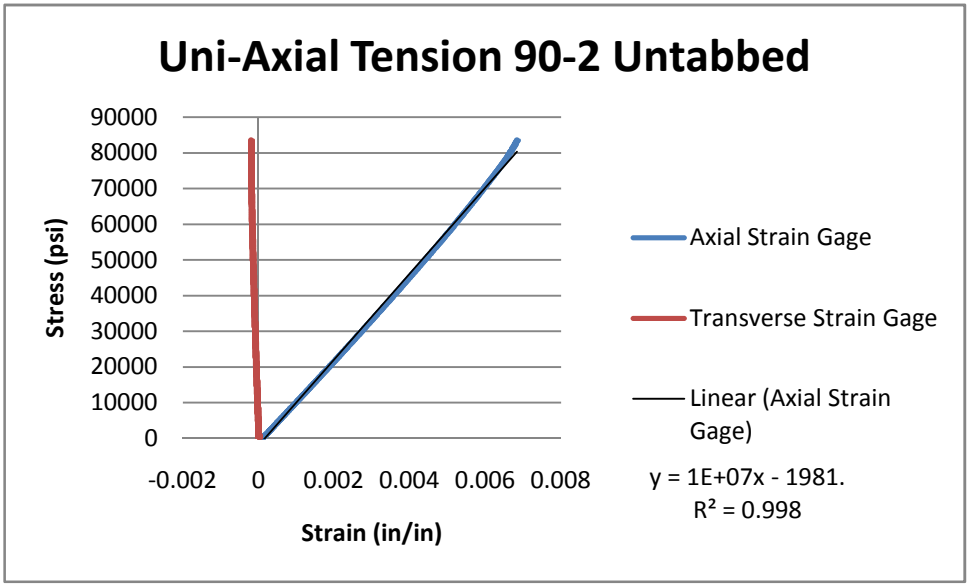

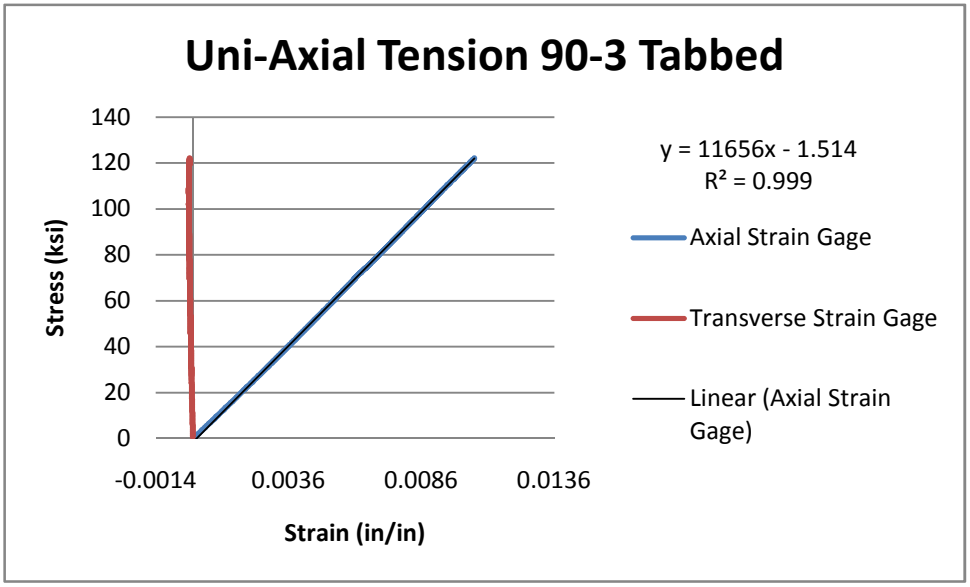

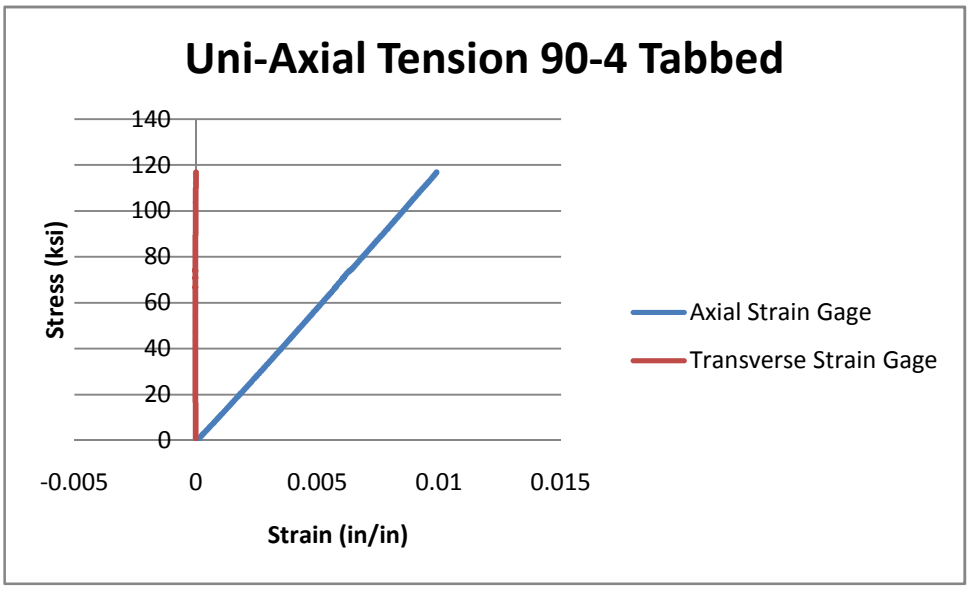

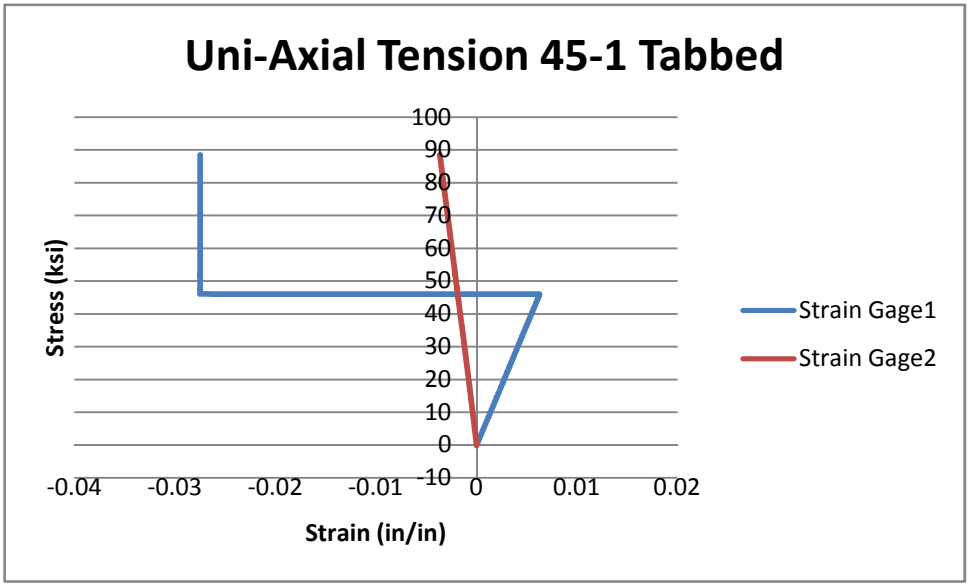

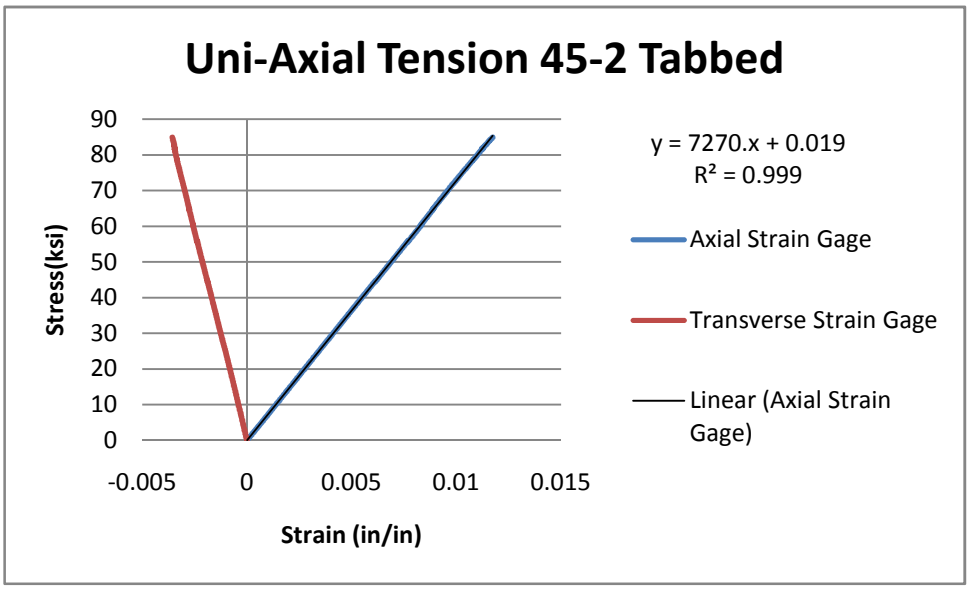

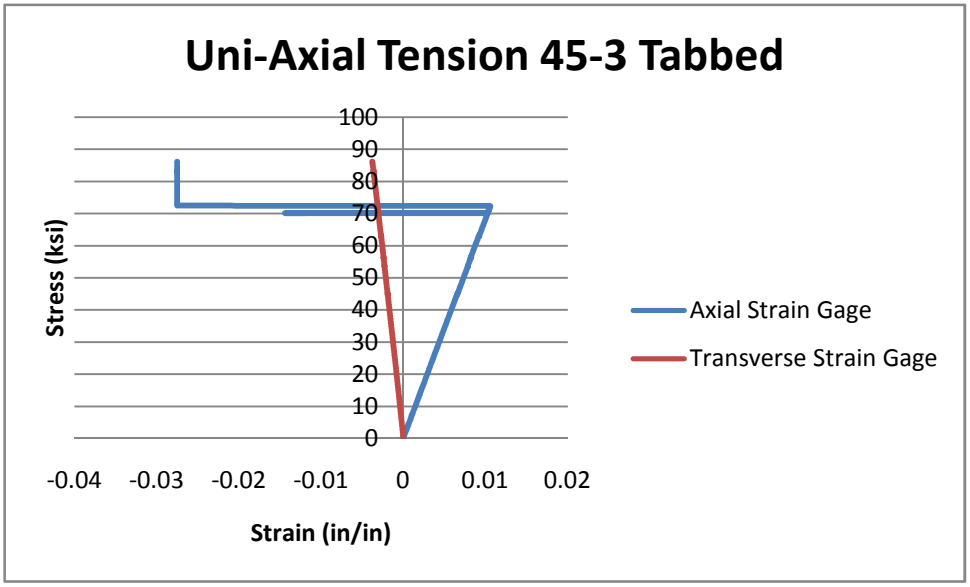

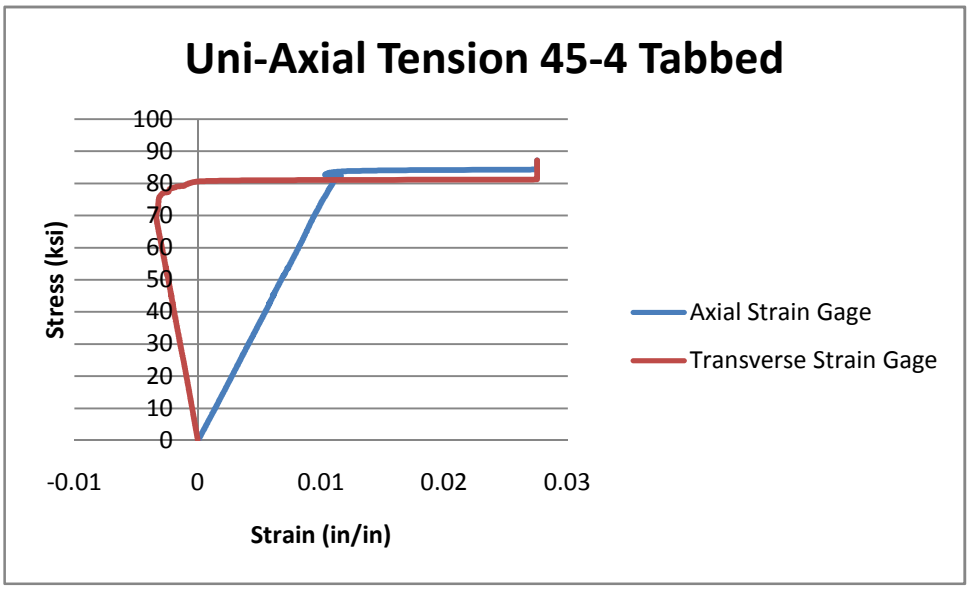

- Young's Modulus$_{45}$=7,200ksi
- Young's Moduls$_{90}$=11,800ksi
- Poisson's Ratio$_{45}$=.3
- Poisson's Ratio$_{90}$=.015
- Fu$_{45}$=85ksi
- Fu$_{90}$=120ksi

APPENDIX B: IM7/PATZ AND G10 MATERIAL PROPERTIES

IM7/PATZ material is the same as IM7/977-2 just made by a different manufacturer. Material properties are from Ash and Welsh [1].

- Mass density = $1.4x10^{-4\ lbf*s\^2}/_{in\^4}$
- Young's Modulus = 25,000ksi
- Poisson's ratio = .3
- Fu=409ksi

G10 material properties [1]:

- Young's Modulus = 2.55Msi
- Poisson's ratio = .4

APPENDIX C: BI-AXIAL TESTS DATA

TYPE I CONTROL:

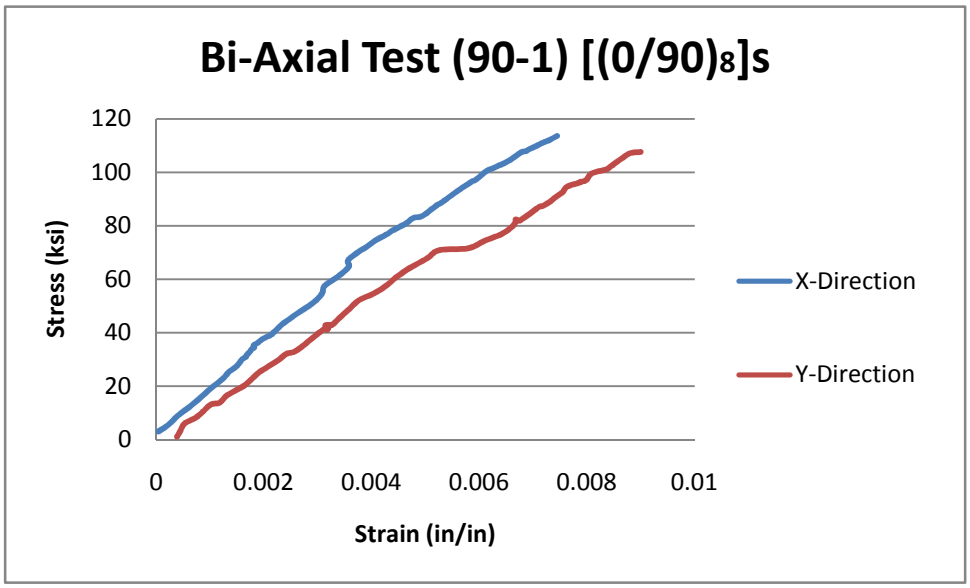

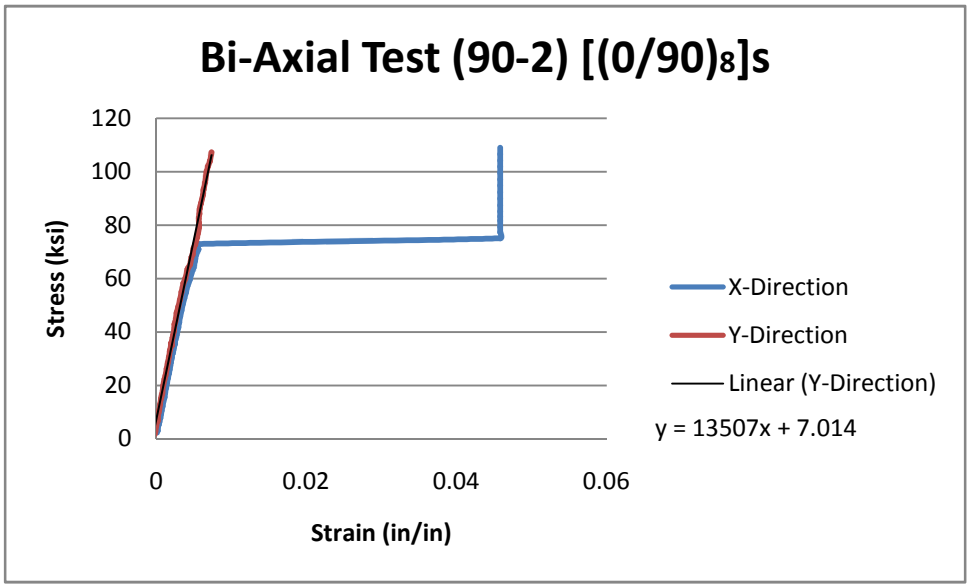

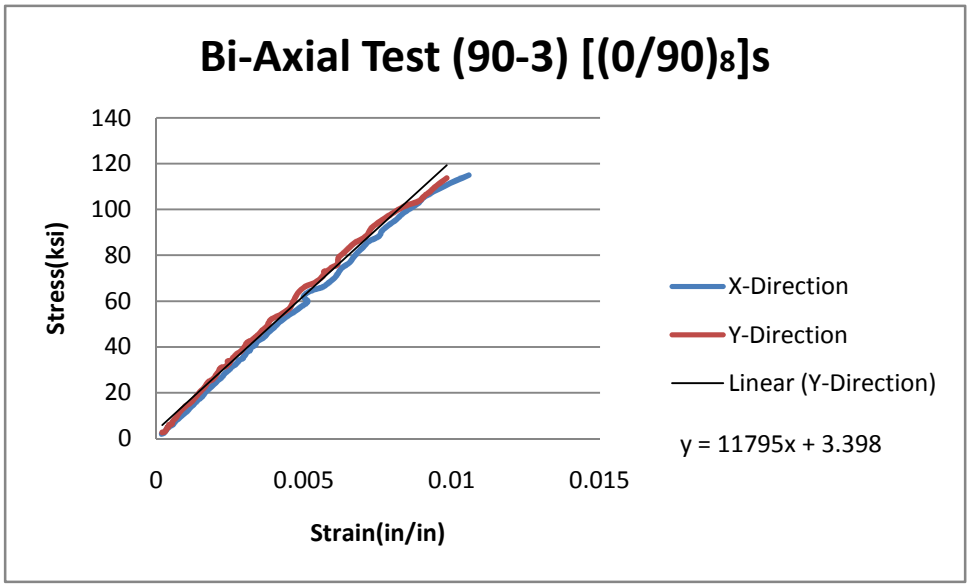

TYPE I TESTS SHIMMED:

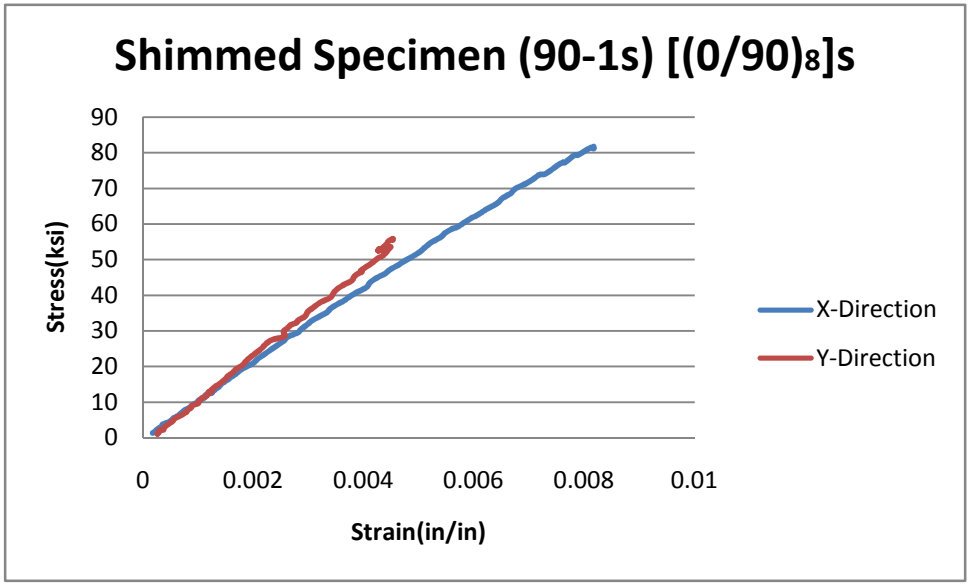

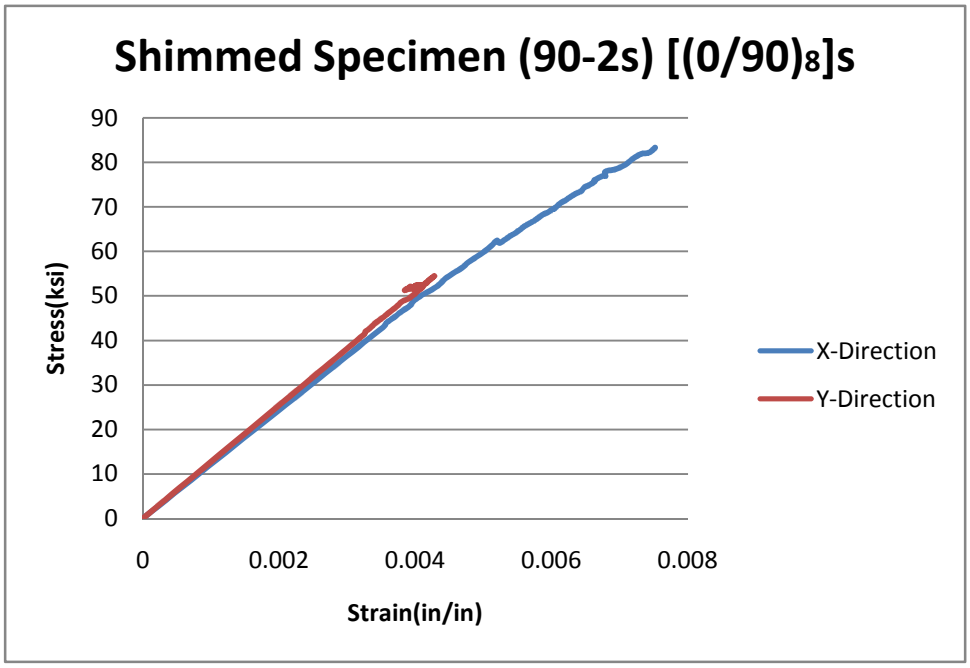

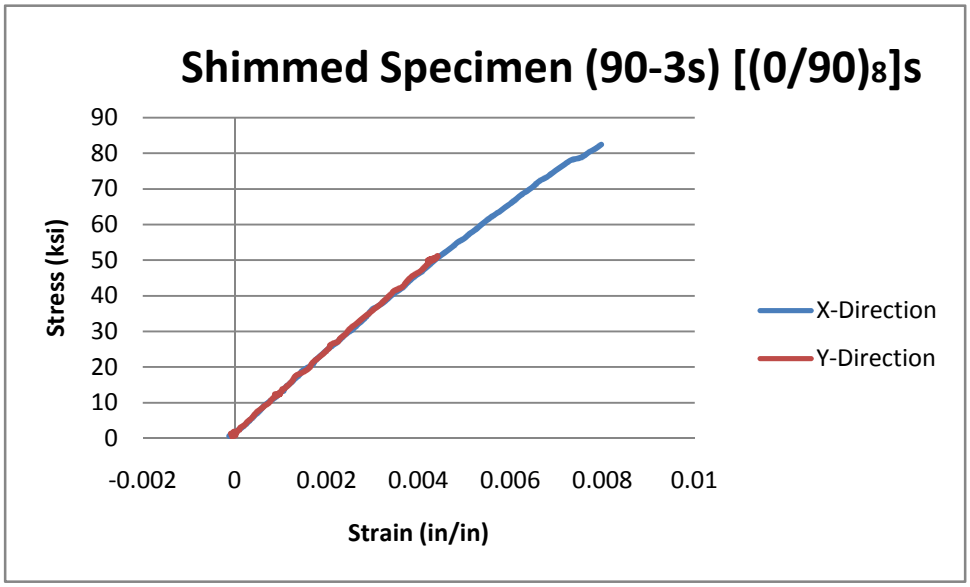

TYPE II CONTROL:

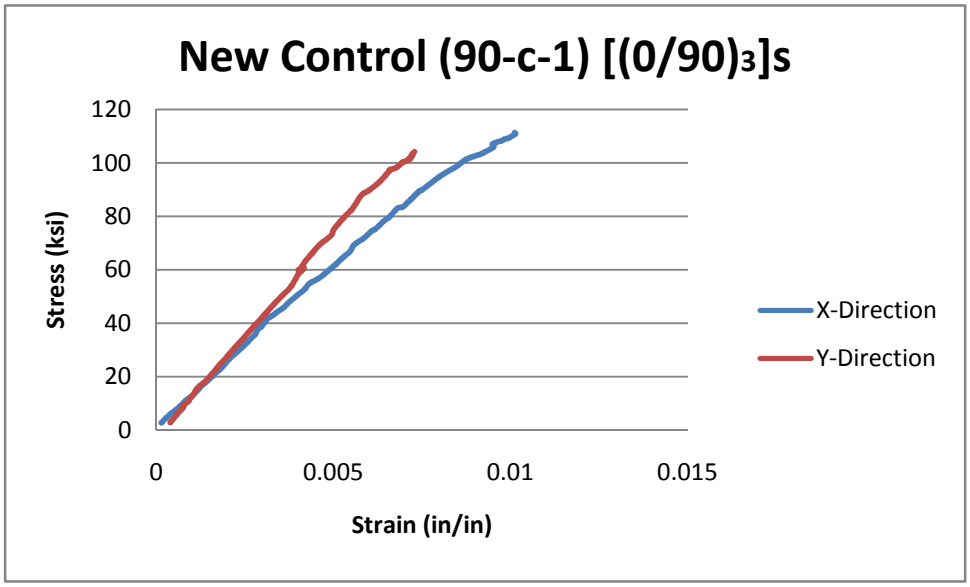

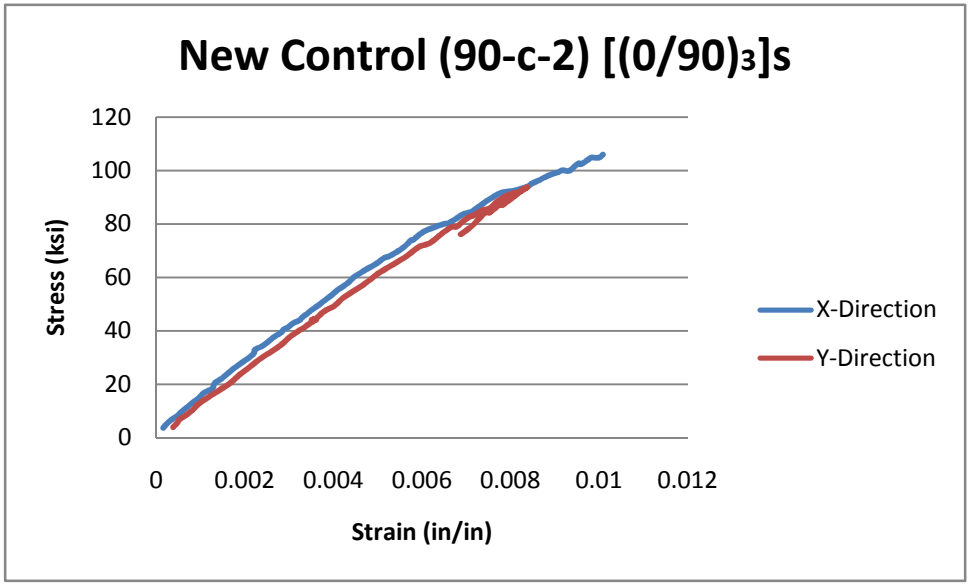

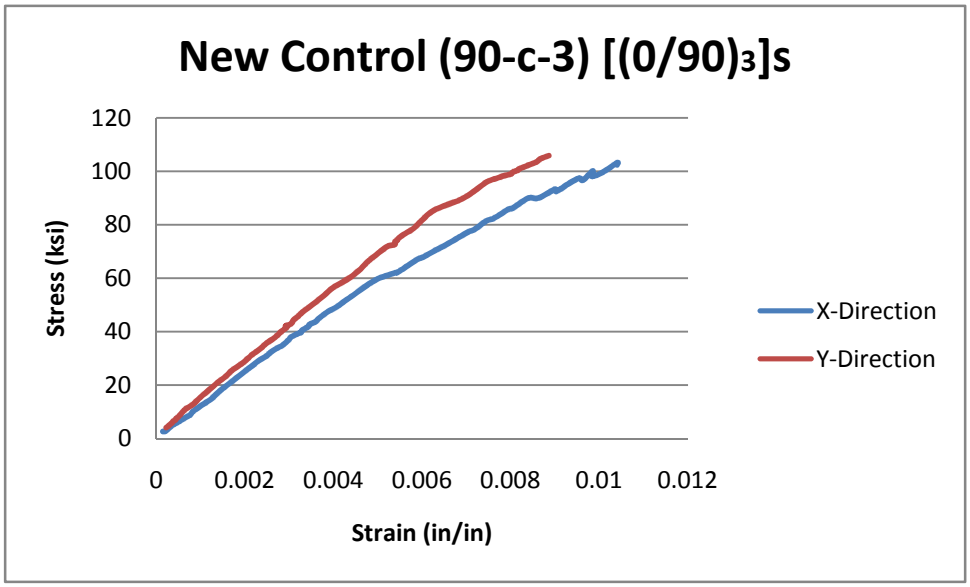

TYPE II BUILT-UP;

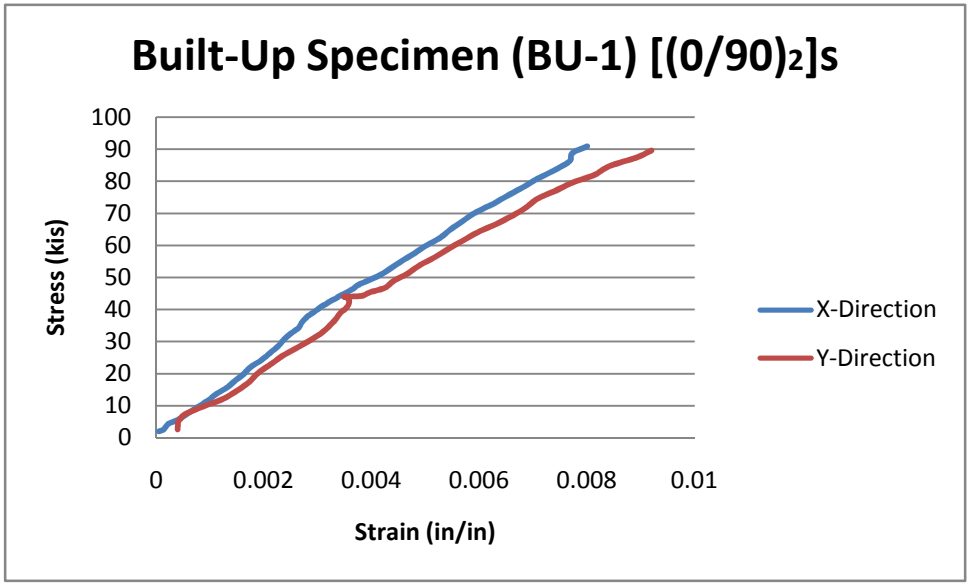

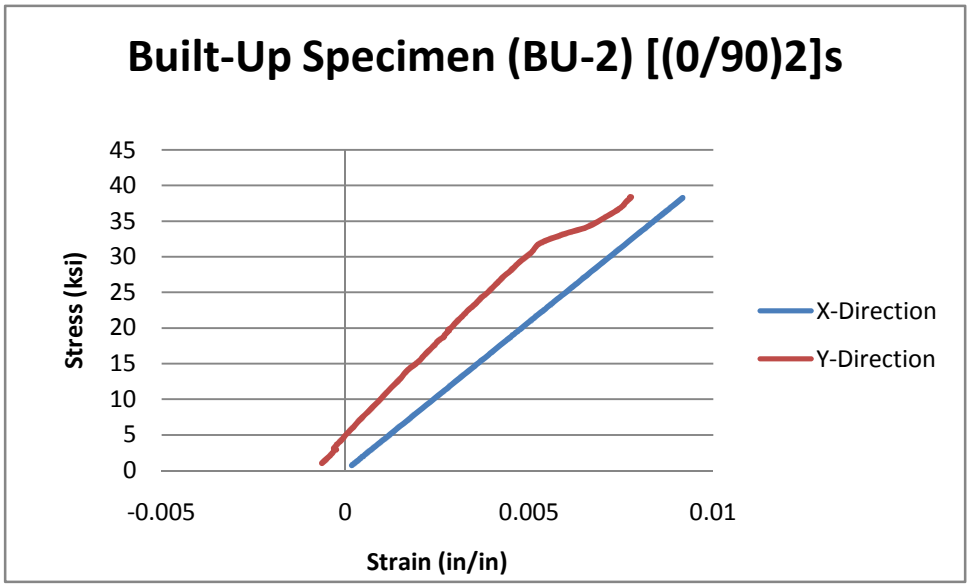

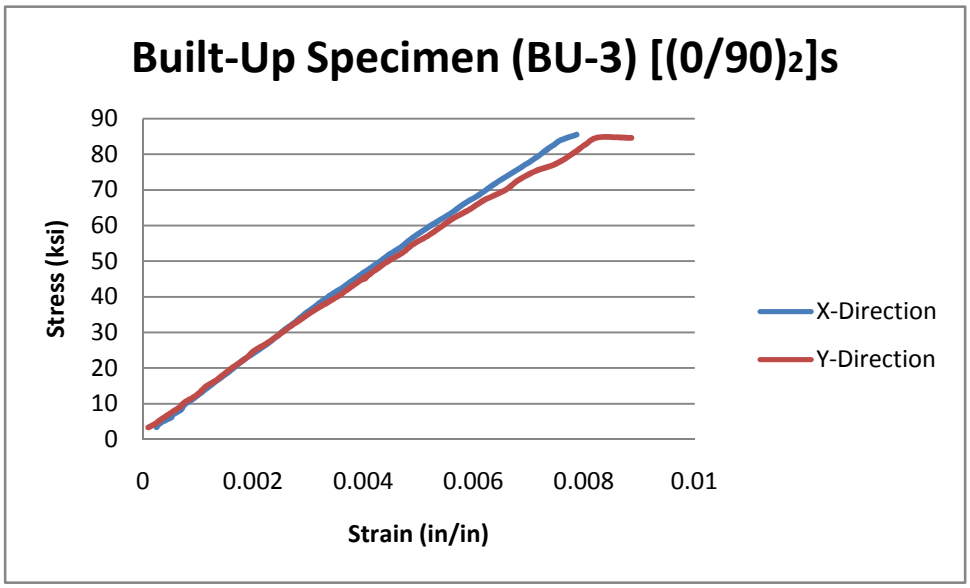

REFERENCES

1. Ash, Jason T. and Welsh, J. S., "Biaxial Strength Measurements of IM7/977-2 Carbon/Epoxy Laminates Using Tabbed Cruciform Specimens," Collection of Technical Papers - AIAA/ASME/ASCE/AHS/ASC Structures, Structural Dynamics and Materials Conference, V2, 2004, pp. 1402-1412.
2. Smits, A., "A Review of Biaxial Test Methods For Composites," Experimental Analysis of Nano and Engineering Materials and Structures, C.35, 2007, pp 933-934.
3. Swanson, S. R., Christoforou A. P., and Colvin G.E. Jr., "Biaxial Testing of Fiber Composites Using Tubular Specimens," Experimental Mechanics, V28.3, 1988, pp. 238-243.
4. Smits, A. and **Van Hemelrijck D., "Design of a Cruciform Specimen for Biaxial Testing of Fiber Reinforced Composite Laminates," Composite Science and Technology, V66 n7-8, 2006, pp. 964-967.**
5. Welsh, J. S., "Development of an Electromechanical Triaxial Test Facility for Composite Materials," Experimental Mechanics, V4.3, 2000, pp. 312-320.
6. Welsh, J. S. and Adams D. F., "An Experimental Investigation of the Biaxial Strength of IM6/3501-6 Carbon/Epoxy Cross-ply laminates Using Cruciform Specimens," Composites Part A: Applied Science and Manufacturing, V33 I6, 2002, pp.829-839.
7. Welsh J. S. and Mayes J. S., "Recent Biaxial Test Results of Laminated Composites and Analytical MCT Predictions," 49th International SAMPE Symposium and Exhibition: Materials and Processing Technology, 2004.

8. Daniel, I. M., "Behavior of Graphite/Epoxy Plates with Holes Under Biaxial Loading, " Experimental Mechanics, V20.1, 1980, pp. 1-8.
9. Jones, D. L., "Effect of Biaxial Loads on the Static and Fatigue Properties of Composite Materials," ASTM Special Technical Publication, 1985, pp. 413-427.
10. "Standard Test Method for Tensile Properties of Polymer Matrix Composite Materials," ASTM D3039, 2006 Annual Book of ASTM Standards, Section 15, Vol. 3, American Society for Testing and Materials, Philadelphia PA, 2006.
11. "Standard Test Methods for Constituent Content of Composite Materials," ASTM 3171, 2006 Annual Book of ASTM Standards, Section 15, Vol. 3, American Society for Testing and Materials, Philadelphia PA, 2006.
12. TCR Composites Data Sheet, Ogden, Utah.
13. "Standard Test Methods for Density and Specific Gravity (Relative Density) of Plastics of Displacement," ASTM D792-86, 2006 Annual Book of ASTM Standards, Section 15, Vol. 08.01, American Society for Testing and Materials, Philadelphia PA, 2006.
14. Edwards, A. L., "Understanding Failure and Damage in Composite Chambercore Structures," University of New Mexico Thesis, 2001.
15. Daniel, Isaac & Ishai, Ori, "Engineering Mechanics of Composite Materials" New York, 1994
16. Pilkey, Walter, "Peterson's Stress Concentration Factors" New York, 1997